

https://dspace.org/

Investigation of the Pt-Al-Cr system as part of the development of the Pt-Al-Cr-Ru thermodynamic database

Suss, Rainer

2008-09-03T11:52:13Z
http://hdl.handle.net/10539/5591

Downloaded from a DSpace repository. https://dspace.org/

PART THREE: THERMODYNAMIC MODELLING IN THE Pt-Al-Cr-Ru SYSTEM USING THERMO-CALC

1. AN INTRODUCTION TO CALPHAD

Phase diagrams are the foundation in performing basic materials research. They are the starting point in the manipulation of processing variables to achieve desired microstructures. Time consuming and costly experimentation is feasible for determining phase equilibria of binaries and ternaries over limited compositional ranges, but not for higher order systems over a wide range of compositions and temperatures. Most real alloys are multi-component, often having more than ten. A good example is nickel-based superalloys (NBSAs). By dint of design, processing and alloy development, extremely complex microstructural systems have allowed NBSAs to attain operating temperatures approaching 90% of their melting point. Up to 15 different elements are mixed within carefully controlled windows of microstructural stability to allow these materials to achieve this balance of structure and properties. Because of this microstructural complexity, it is difficult to carry out further development of NBSAs - or other complicated alloy systems - by purely empirical means. Alloy development costs and time can be significantly reduced by employing computational thermodynamics whereby, using appropriate thermodynamic databases, multiphase multicomponent equilibria can be predicted. This has given rise to large and sophisticated data bases that allow mathematical modelling to go hand in hand with experimental design.

The method employed is called CALPHAD - Calculation of PHAse Diagrams. The calculations are based on Gibbs Free Energies as functions of temperature, pressure and compositions for each pure element and individual phase in a system. The basis for the construction of the database is the provision of reliable thermodynamic models for the unary (pure elements) and binary systems within the database. It relies on critical assessment of the experimental information available for each system, and by the application of appropriate models for each of the phases involved, model parameters are derived. It is often necessary to critically assess the higher order systems as well, typically the ternary systems and on occasion, quaternary systems, should such information be available. The success of the CALPHAD technique depends upon the reliability of these databases. The Gibbs Energies of multicomponent alloy phases can be obtained from the lower order systems via extrapolation

(usually the Muggianu method [1975Mug]), enabling the calculation of (in many instances) reliable higher order phase diagrams. Experimental work should then only be required for confirmatory purposes, and not for the determination of whole diagrams.

The basic methodology of thermodynamic database design, construction and optimisation has been described in detail many times, for example by Hari Kumar et al. [2001Har] and more recently Schmid-Fetzer et al. [2007Sch]. Only a brief overview is given here.

The temperature dependence of the Gibbs energy is described by:

$$G(T) = A + BT + CT\ln T + \sum DT^n$$

where *A-D* are adjustable parameters. The compositional dependence of a binary substitutional solution phase (eg. liquid, fcc, bcc, hcp…)) ϕ, of components *i* and *j,* is given by:

$$G_m^\phi = x_i {}^O G_i^\phi + x_j {}^O G_j^\phi + RT(x_i \ln x_i + x_j \ln x_j) + {}^E G_m$$

where the ${}^O G$ terms are the 'so-called' lattice stability terms, $RT(x_i \ln x_i + x_j \ln x_j)$ denotes the entropy contribution treated by the Bragg-Williams approximation (assuming random mixing of *i* and *j*) and the ${}^E G$ term is the excess Gibbs energy of mixing. The excess Gibbs energy is described by the 'Redlich-Kister' polynomial [1948Red]:

$${}^E G_m = x_i x_j \sum_{n=0} {}^n L(x_i - x_j)^n$$

where L is *nth* interaction parameter between the i and j atoms and can be temperature dependent in the form

$${}^n L = a_n + b_k T + c_k T \ln T$$

where a_k, b_k and c_k are model parameters to be determined from experimental data.

These models are not good enough for higher solute contents or systems that show ordering. The Sub Lattice model (SL) or Compound Energy Formalism (CEF) was developed by Hillert and co-workers [1970Hil, 1981Sun, 1986And]. It entails interlocking sublattices on which the various components can mix. Elements allowed in a sublattice are those found in actual crystallography. The structure of a phase is represented by the formula, e.g.

$(A,B)_k(D,E,F)_l$ where A and B mix on the first sublattice and D, E and F on the second. *k* and *l* are stoichiometric coefficients. A number of standard 2/3/4 SL-CEF models have been developed to describe order-disorder transformations.

Prior to building a database, it must be known which phases need descriptions. The elemental information, and any phase that is already included in the SGTE database [1991Din], can be accessed from that database. (SGTE, *Scientific Group Thermodata Europe*, is an international organisation collaborating on databases.) For phases that are not represented by the SGTE database, a number of factors must to be taken into consideration. Firstly, the structure of the phase has to be decided, including the number of sites for the atoms, and which particular atoms fit on the sites. Each phase is modelled with sublattices, and each sublattice usually corresponds to a type of atom position. This information is usually derived from (XRD) structural information and composition ranges, and is usually made to be as simple as possible. Next, some values have to be obtained for the interaction parameters. The interaction parameters can be guessed for an initial value, or set to zero, and the user can decide which parameter can be changed during optimisation. In optimisation, experimental data is compared against the thermodynamic description and the thermodynamic description is adjusted to best fit the experimental data. Optimisation is an iterative process whereby selected expressions of the thermodynamic descriptions are allowed to change so that the agreement with the experimental results is improved.

2. AN INTRODUCTION TO THERMO-CALC

The databases are linked to software for the calculation of phase equilibria for applications of interest. Such software packages include Thermo-Calc [1985Sun, 2002And], FactSage [1977Tho, 1990Eri, 2002Bal], MTDATA [1989Din, 2002Dav] and PANDAT [2002Che]. These different packages have been described in depth in a special issue of the CALPHAD Journal [**26**(2) (2002) 141-312].

Thermo-Calc is a powerful and flexible software package for a variety of thermodynamic and phase diagram calculations based on a powerful Gibbs Energy Minimiser. It has gained reputation wordwide as one of the best software packages for such calculations. Thermo-Calc can use many different thermodynamic databases, especially those developed by SGTE. General Databases with data for compounds and solutions include:

- SSUB: SGTE Substances database. Data for 5000 condensed compounds or gaseous species.
- SSOL: SGTE Solutions database. A general database with data for many different systems covering 78 elements and 600 solution phases.
- BIN: SGTE Binary Alloy Solutions database.

There are also other commercially available databases for specific alloy systems, eg. TTAl (aluminium), TTMg (magnesium), TTNi (Ni-based superalloys), TCFe (steels and ferritic alloys), TTTi (titanium) and SNOB (Spencer's Nobel Metals database).

Thermo-Calc consists of several modules for specific purposes and the various tasks the user may be interested to perform. The TDB module is used for retrieving databases or data files. The GES module is used for listing system information and thermodynamic/kinetic data, or interactively manipulating and entering such data. The POLY module can calculate various complex heterogeneous equilibria, while the POST module makes it possible to plot many kinds of phase- and property diagrams. The PARROT module provides a powerful and flexible tool for data evaluation and assessment of experimental data (used in the above-mentioned optimisation phase), whereby the Gibbs energy functions can be derived by fitting experimental data by a least squares method.

3. MOTIVATION FOR THE DEVELOPMENT OF A THERMODYNAMIC DATABASE FOR Pt-CONTAINING ALLOYS

The need for a predictive thermodynamic database for Pt-containing alloys was identified at the outset of the alloy development programme. It was envisaged that, like the NBSAs, the Pt-alloys would be multicomponent, 5th order or above, and that it would not be viable to determine all the phase equilibria via experimental means. The database will aid the design of alloys by enabling the calculation of the composition and proportions of phases present in high order alloys of different compositions.

Since the basis of the alloys is the Pt_{84}:Al_{11}:Ru_2:Cr_3 alloy, the thermodynamic database had to be built on the Pt-Al-Cr-Ru system. It was soon realised that the SGTE databases had all the stable elements and the most common and well-known systems, i.e. those that are industrially important, but comprised few of the required Pt phases. For example, the intermetallic phases

in the Al-Ru and Pt-Al systems are not included in the SGTE database. Even the database for noble/precious metals (Spencer's) is not complete for the purposes of this investigation - it does not contain all the elements of interest for this study, nor all the phases. If there is no description for a particular phase, then the calculated phase diagram cannot include it.

For Pt alloys there were much less experimental data and few accepted ternary systems. Even some of the binary systems have problems. Thus, part of this work included the study of phase diagrams to address the lack of data, and to use these data to compile the thermodynamic database.

The assessment of the Pt-Al-Cr-Ru system started by studying the four component ternary systems: Al-Cr-Ru [2000Com1, 2000Com2, 2001Com]), Pt-Cr-Ru [2002Süs1, 2003Süs1, 2003Süs2, 2004Süs1, 2006Süs1], Pt-Al-Ru [2002Pri2, 2005Pri], and Pt-Al-Cr (this thesis). Studies of as-cast alloys were done to determine the solidification reactions and liquidus surface. The samples were also heat-treated at 600° and 1000°C and then analysed so that the phase compositions at known temperatures could be input to Thermo-Calc. The complete ternary systems were determined so that the complete systems could be optimised in Thermo-Calc. The reason for this, rather than optimising portions of them, is that there were very little data available for the systems, and any thermodynamic model needs to be valid over the complete range of compositions in the base system before adding the minor components. If only a small region was to be optimised (e.g. the region between the (Pt) and Pt_3Al phases only), then it was likely that although the model would be sufficiently good locally, when new elements were added, or other elements added beyond their original compositions, the fit would either be very erratic or the calculations would not be able to converge.

4. BUILDING THE DATABASE

The relevant binaries are optimised first. Once each binary system is modelled satisfactorily, they can be added to form the ternary systems, after which each ternary system must be optimised individually. This is done using the data derived experimentally within the research programme.

A very good summary of the modelling work done is given in a recent review paper by Cornish et al. [2006Cor]. A model for the ternary system Pt-Al-Ru (the calculated diagram shown in Figure 3.1) was completed by Prins et al. [2003Pri, 2004Pri], its optimisation based on experimental work by Prins et al. [2005Pri]. The Al-Cr-Ru system will be addressed in the near future.

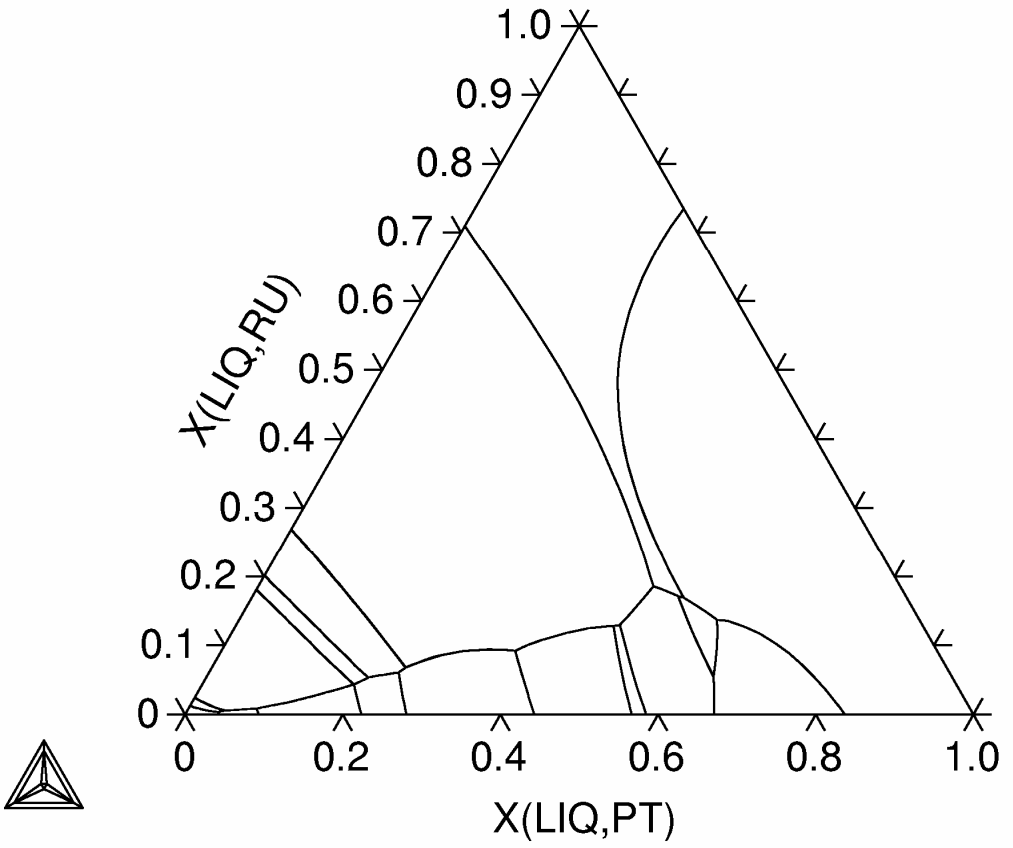

Figure 3.1. The Pt-Al-Ru liquidus surface projection as calculated by Prins et al. [2003Pri].

Cr-Pt-Ru was modelled earlier by Glatzel and Prins [2003Gla], but based on models for Pt-Cr and Cr-Ru that were heavily criticised at the 2004 Calphad Conference [2004Süs2] (Part 3, §4.3). Therefore the system had to be revisited, especially because more phase data had become available [2004Süs1, 2006Süs] since the initial assessment that would make optimisation easier. This was done recently by Watson, Cornish and Süss [2006Wat], and it was also good preparation for the modelling of Pt-Al-Cr which is a much more complicated system.

A different approach was taken than before. The optimisation for Cr-Pt of Oikawa el. [2001Oik] was accepted in the work and no attempt was made to introduce $CrPt_3$. For Cr-Ru, Gibbs energy parameters for the bcc, hcp, sigma and A15 phases were optimised using WinPhad together with the invariant temperatures and compositions taken from Massalski [1990Mas]. The fit of the calculated phase diagram to the experimental invariants was much better than that of Glatzel [2003Gla]. The model used for A15 Cr_3Ru was compatible with that used for the A15 Cr_3Pt in case the phase is actually contiguous across the ternary. So far, experimental results at Mintek of alloys in the as-cast condition or annealed at 600°C or 1000°C were inconclusive in showing whether the phases are contiguous. Annealing samples of intermediate compositions between Cr_3Ru and Cr_3Pt at ~850°C (a temperature the phases should meet if they were contiguous) was also inconclusive. A Pt-Ru phase diagram, optimised using WinPhad and calculated using Pandat, was in good agreement with that given by Massalski [1990Mas].

The thermodynamic description of the ternary system was optimised against the experimental data of Süss et al. [2006Süs] and Zhao [2004Zhao] (Figure 3.1). The assessment module of *MTDATA* was used to perform the optimisation.

It was found that a reasonable fit to the ternary experimental data available in the literature could be achieved by producing a suitable description for the metastable binary Cr-Pt hcp phase. The calculated diagram for 1000°C is given in Figure 3.2. Most improvement to the calculated diagram would be achieved by improvement to the description of the A15-phase. Destabilising the Cr_3Ru A15-phase in the Cr-Ru binary would have the effect of reducing the extension of the A15 phase into the ternary, which is desirable, but this would of course, have implications with respect to the Cr-Ru phase diagram. Improvement to the modelling of this phase in the binary system would undoubtedly improve the overall modelling of this phase, but this would require further experimental study. Not only is the contiguity question of Cr_3Ru and Cr_3Pt important, but the Cr-Ru system in itself shows many other unknowns. Undertaking slow scan DTA for temperatures of formation and dissolution for the intermetallic compounds is very necessary. Using the sigma model for Cr_2Ru would also be preferable.

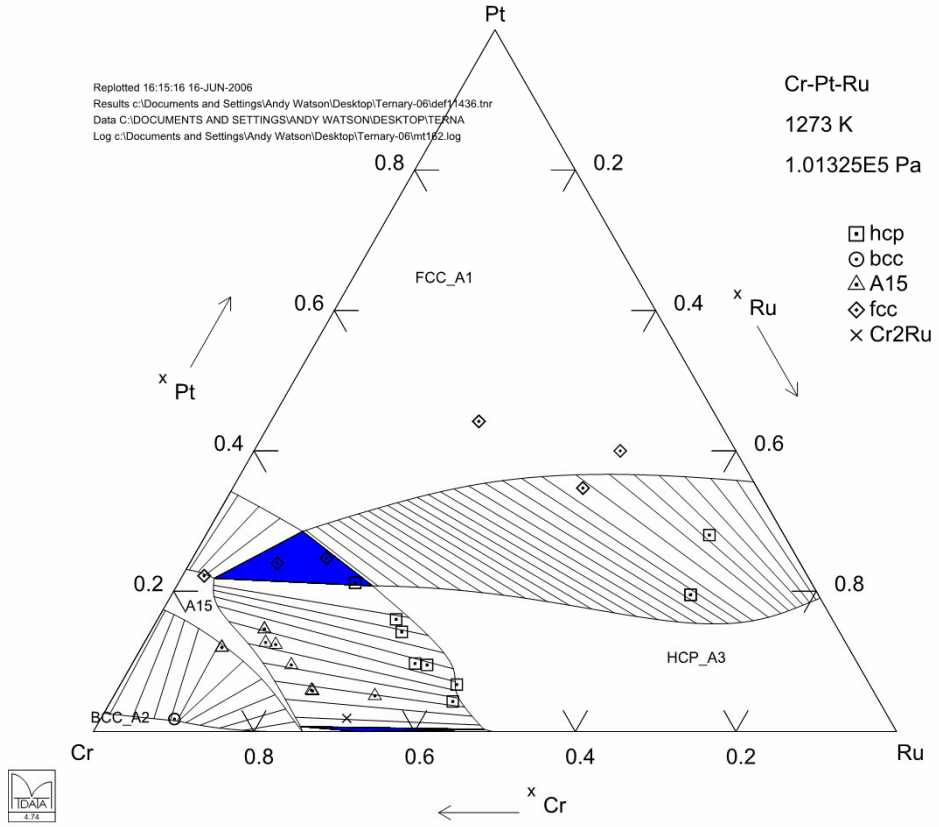

Figure 3.2. Calculated isothermal section for the Cr-Pt-Ru system for 1000°C [2006Wat] with experimental data from [2006Süs2].

The Pt-Al-Cr system was modelled next. Since this thesis is focussed on the Pt-Al-Cr system, a detailed description of its modelling will be given in the next sections.

Since Pt-Al-Cr comprises three binary systems, Pt-Al, Al-Cr and Pt-Cr, the first step was to model these three systems separately. This was done using Thermo-Calc Classic Version Q.

4.1 Pt-Al

Information on the phase equilibria in the Pt-Al system is given in Part 1 §2.2.

Initially, the four sublattice compound sublattice formalism (4SL-CEF), a version of the compound energy formalism model [1998Sun], was used, which models different combinations of four atoms of two different elements, for example: (A) (mathematically A_4), A_3B, AB (mathematically A_2B_2), AB_3 and (B) (mathematically B_4) where at least two of

these appear in a system. This method was used for the (Pt) and Pt_3Al phases, because this model had used in the development of the nickel-based superalloy database [1997And, 2001Dup].

However, when the 4SL-CEF model was applied to the Pt-Al system [2002Pri1], the results were less successful, mainly because there were very few data, and the system was more complex. The intermetallic compounds $Pt_{21}Al_5$, $Pt_{21}Al_8$, $PtAl_2$, Pt_2Al_3, PtAl, Pt_5Al_3 and Pt_2Al were treated as stoichiometric compounds. The β phase was assumed to be stoichiometric, since very little experimental information was available, and was treated as $Pt_{52}Al_{48}$.

The work by Prins et al. was re-created. The calculated phase diagram, shown in Figure 3.3(a), appears to agree with the experimental diagram, shown in Figure 3.3(b) for easy reference. However, the 4SL-CEF model did not give the differently ordered Pt_3Al phases. The calculated compositions and temperatures for the invariant reactions of the intermetallic phases are in general good agreement with the experimentally reported compositions and temperatures. The congruent formation of the Pt_3Al phase and $L \rightarrow Pt_3Al$ + (Pt) eutectic reactions are not in very good agreement with the experimental diagram, as both reactions are shifted to lower platinum compositions in the calculated system. The β phase calculated with this particular database was stable down to 1000° C, which was incorrect, compared to the experimental diagram.

The congruent formation of the Pt_3Al phase and $L \rightarrow Pt_3Al$ + (Pt) eutectic reactions are not in very good agreement with the experimental diagram, as both reactions are shifted to lower platinum compositions in the calculated system. The 4SL-CEF model is such that the formation composition of Pt_3Al is fixed at 75 at. %, while it has been reported in the literature to form congruently at 73.2 at. %. This off-stoichiometry formation cannot be described with the model, and subsequently had an influence on the temperature as well as the enthalpy of formation for the Pt_3Al phase. The symmetry and fixed compositions of the 4SL-CEF model made it also difficult to fix the eutectic reaction to lower Pt contents in the calculation. Furthermore, the phase area of the (Pt) solid solution is too narrow, especially at lower temperatures, although the phase area for the Pt_3Al phase is acceptable. However, the Pt_3Al phase is ordered throughout its phase area and the unstable $PtAl_3$ ($L1_2$) and Pt_2Al_2 ($L1_0$)

phases, which are introduced through the 4SL-CEF model, are not stable at any composition or temperature in the phase diagram, which is correct.

This model was used in this investigation. Further work on this system was postponed until more data to describe the (Pt) and Pt_3Al phases has been obtained. Currently, the Pt-Al binary is being investigated with the advent of Mintek's new Nova NanoSEM, and good results are being obtained [2006Tsh]. The data from these alloys will be used to optimise the Pt_3Al phase in the Pt-Al binary at a later stage.

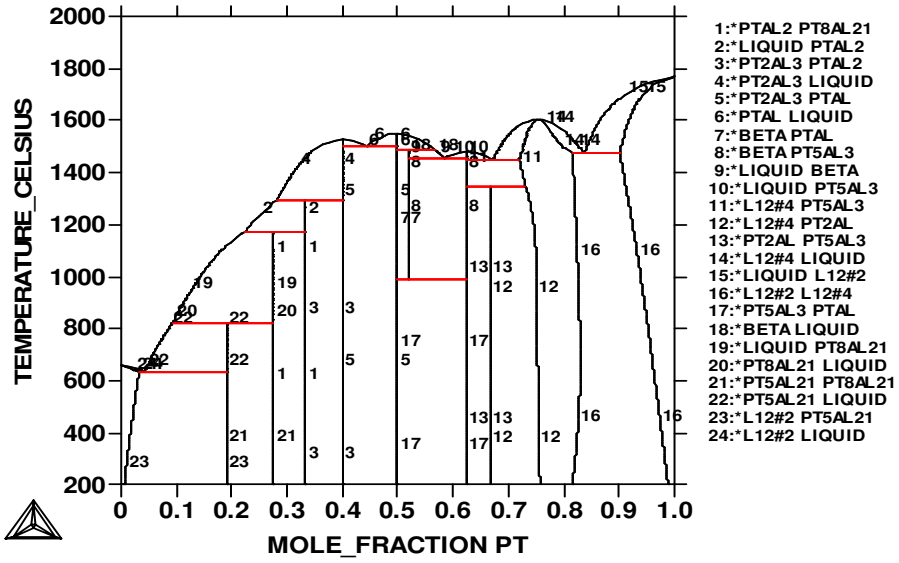

(a)

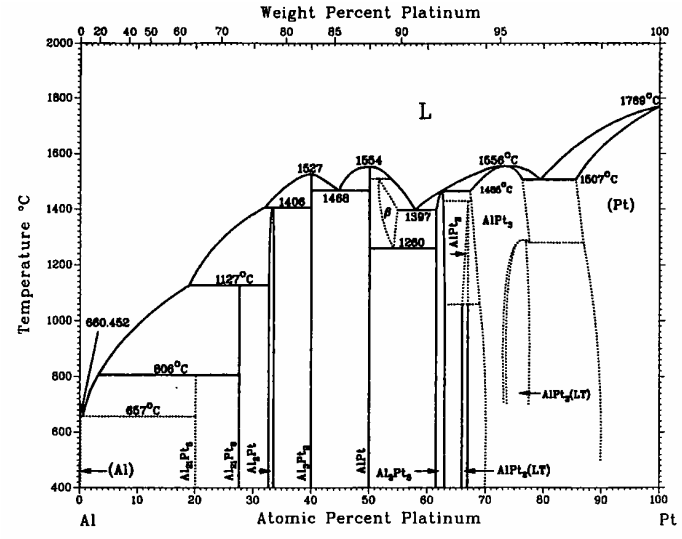

(b)

Figure 3.3. Comparison of Al-Pt phase diagrams: a) Calculated using data from Prins [2004Pri]; b) Experimental [1990Mas].

4.2 Al-Cr

Information on the phase equilibria in the Al-Cr system is given in Part 1 §2.3.

Using data from the COST database [1998Ans], the binary phase diagrams for Al-Cr was calculated (Figures 4.4(a)). When compared to the published phase diagram (shown again for easy reference in Figures 4.4(b)), it can be seen that the modelled diagram is in very good agreement. These data for Al-Cr were used throughout.

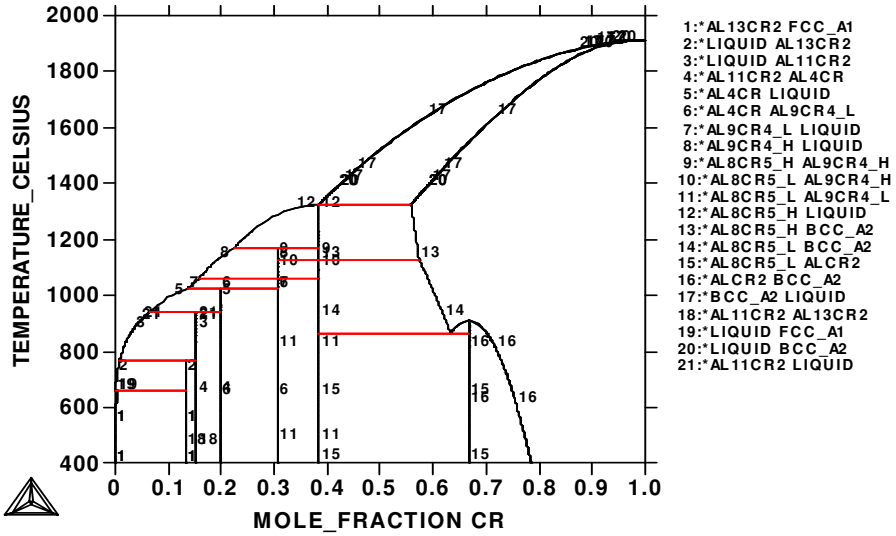

(a)

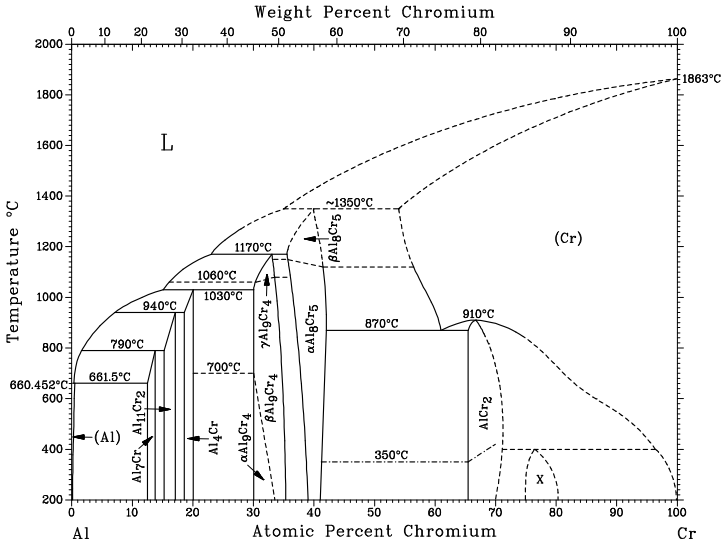

(b)

Figure 3.4. Comparison of Al-Cr phase diagrams: a) Calculated using data from COST [1998Ans]; b) Experimental [1990Mas].

4.3 Cr-Pt

Information on the phase equilibria in the Cr-Pt system is given in Part 1 §2.1.

As mentioned before, the first Pt-Cr assessment done within this work (Figure 3.5(a), [2003Gla]) built on the original assessment of Oikawa *et al.* (Figure 1.3, [2001Oik]). It incorporated the 4SL-CEF model to the fcc phases, (Pt), Pt_3Cr and PtCr, to give a worse fit to the currently accepted phase diagram (Figure 3.5(b), [1990Mas]) than the work of Oikawa *et al.* There were many problems with using the 4SL-CEF model, mostly because the model is complex and requires data - which were not available - for the different phase types that might be probable, and if the phases do not exist naturally, the only way that these data can be obtained is by *ab initio* techniques.

A new approach was initiated: that the phase diagram of Oikawa et al. [2001Oik] would be recreated and this assessment only changed when there were good experimental reasons for thus doing. Oikawa et al. has shown before that the eutectic temperatures for Pt-Cr are reversed to those given by Massalski [1990Mas]. This was confirmed by experimental evidence found at Mintek in the ternary systems Cr-Pt-Ru [2006Süs1], Al-Cr-Pt [2005Süs] and Cr-Ni-Pt [2005Nzu]. Until experimental results show otherwise, the assessment of Oikawa et al. would be used and extrapolated into the ternary. However, Oikawa's model does not include the ordered $L1_2$ Pt_3Cr and $L1_0$ PtCr phases, and these had to be added.

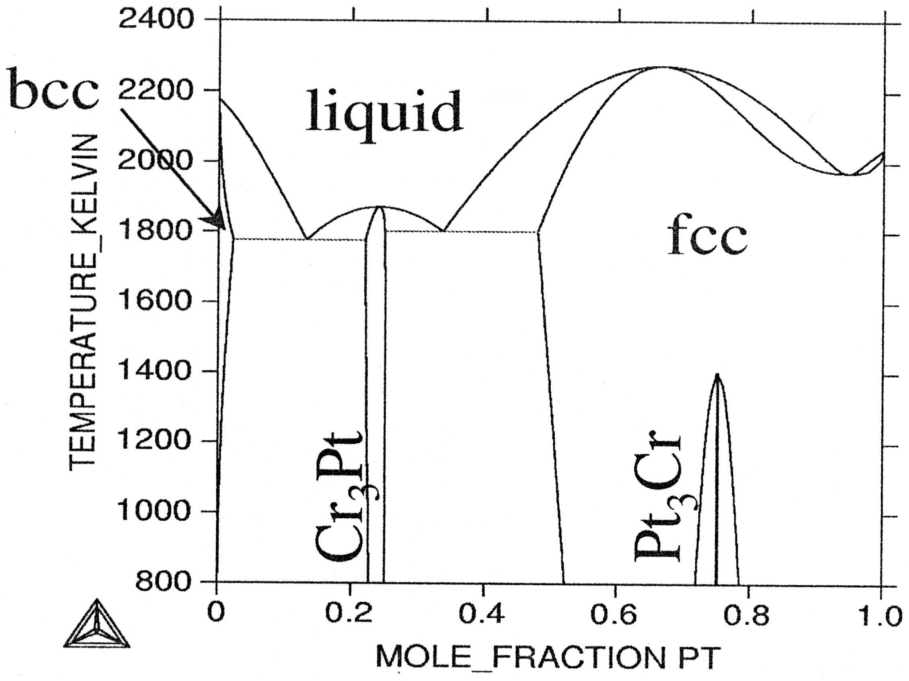
bcc
liquid
fcc
Cr_3Pt
Pt_3Cr
TEMPERATURE_KELVIN
MOLE_FRACTION PT
2400
2200
2000
1800
1600
1400
1200
1000
800
0
0.2
0.4
0.6
0.8
1.0

(a)

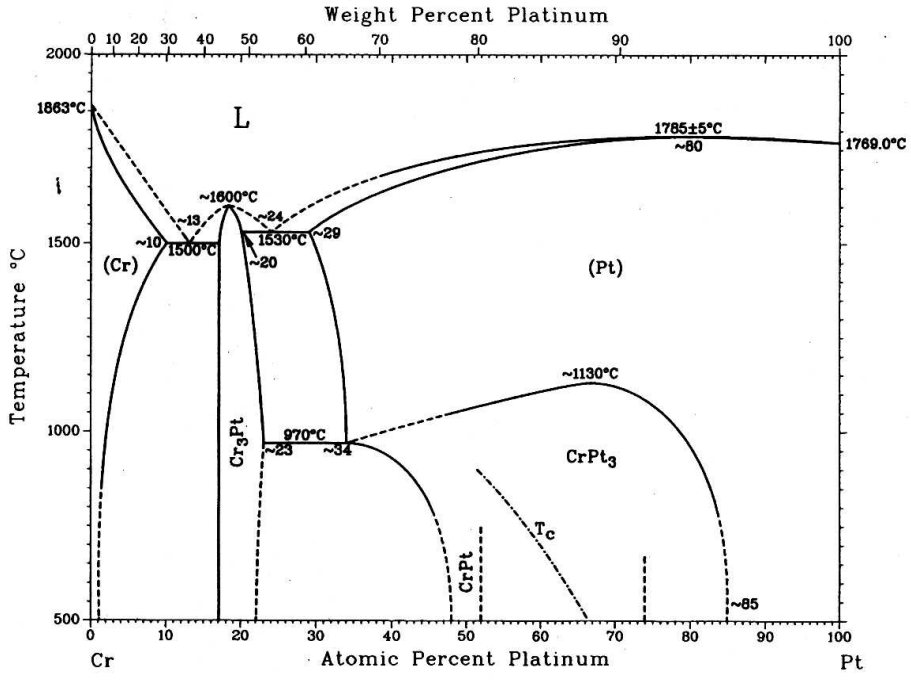
Weight Percent Platinum
Atomic Percent Platinum
Temperature °C
Cr
Pt
L
(Cr)
(Pt)
1863°C
1769.0°C
1785±5°C
~80
~1600°C
~13
~24
~10
1500°C
1530°C
~29
~20
~1130°C
970°C
~23
~34
Cr_3Pt
$CrPt_3$
CrPt
T_c
~85

(b)

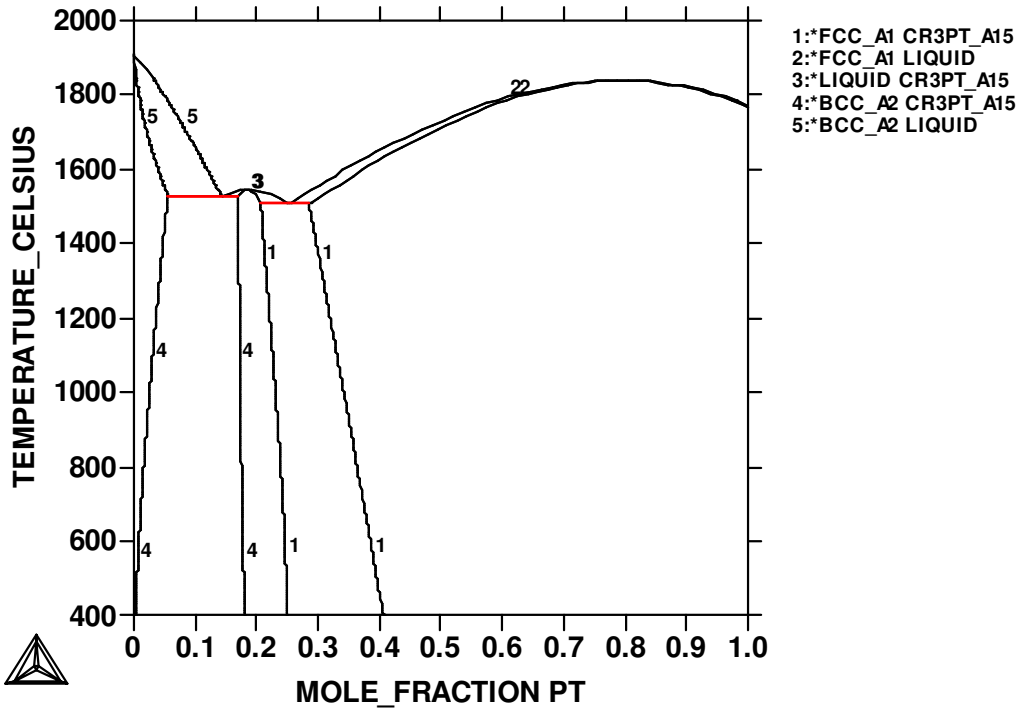

(c)

Figure 3.5. Comparison of Cr-Pt phase diagrams: a) Calculated initially by Glatzel et al. [2003Gla]; b) Experimental [1990Mas]; c) Re-created based on the work by Oikawa et al. [2001Oik].

The question arose whether to use a complex model or not. In general, it is best to have the simplest models possible, because then fitting is easier and probably more meaningful. This is especially so when the data are limited. There are commercial databases available with very simple modelling, and these are very useful. One would think that a simple model for the Pt-Cr system would suffice. However, since the disordered fcc phase (Pt) in Pt-Al is already modelled using the 4SL-CEF model, one would have to do the same for (Pt) in Pt-Cr, to make the models compatible. Only then can the assessment be extrapolated into the ternary.

The 4SL-CEF model was therefore also used for the fcc phases (Pt), Pt_3Cr and PtCr. The modelled diagram is shown in Figure 3.6(a). The results were similar to those of Preussner et al. (Figure 3.6(b), [2006Pre]), who used end points calculated using *ab initio* techniques, but deemed more comparable to the accepted published diagram (Figure 3.5(b)), because Preussner et al. incorporated a stable $L1_2$ structure at 63 at.% Cr discovered by Greenfield and Beck [1956Gre] that is normally not shown in experimental phase diagrams.

New work by Zhao et al. [2005Zha] has shown different and more realistic ordering ranges (Figure 1.2), and this could be incorporated into the system in future if corroborating evidence arises.

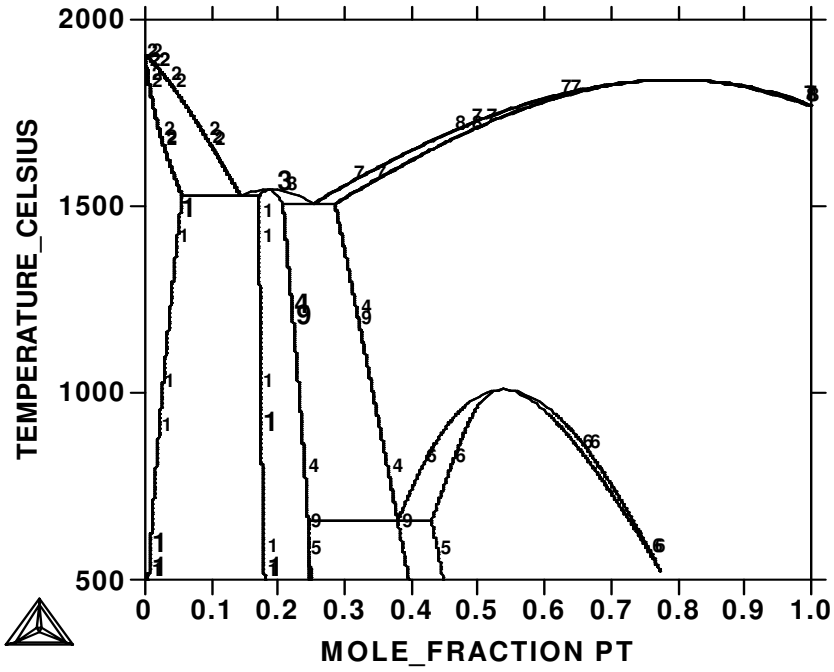

(a)

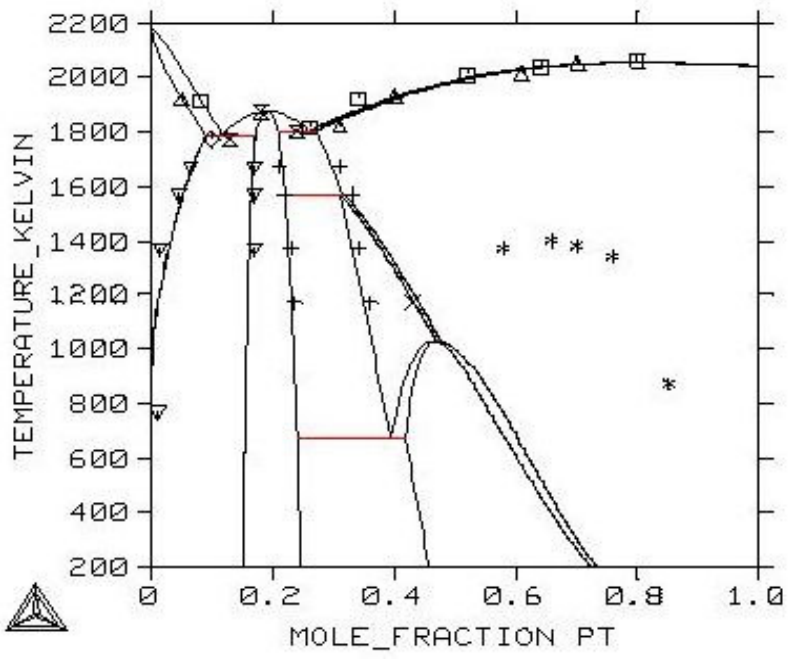

(b)

Figure 3.6. Comparison of Cr-Pt phase diagrams: a) Updated calculation (this work); b) Calculated by Preussner et al. [2006Pre].

4.4 Pt-Al-Cr

4.4.1 Extrapolation

In order to model the Pt-Al-Cr system, the three binary systems had to be added together. In theory, the binary database files should just be copied into a single file, and the ternary database would be complete. However, this hardly ever the case, and especially so for Pt-Al-Cr, because the system has ternary phases that needed to be incorporated into its model.

As a starting point, the three databases were simply added, repetition deleted and checked for consistency. It did not yield good results. The major problem initially was the presence of the ordered $L1_2$ Pt_3Al phase in the Pt-Al system, and the ordered $L1_2$ Pt_3Cr and $L1_0$ PtCr phases in the Pt-Cr system, that were described as separate composition sets (Table 3.1). Figure 3.7 shows the best extrapolation-only of the binary databases at 1000°C, and from the fact that liquid extended from the (Al) to the (Pt) corner (i.e. Pt with melting point of 1768°C liquid at 1000°C - which was totally wrong) it was clear that the description for the fcc phases (disordered and ordered) was incorrect. The fact that there were several error messages from Thermo-Calc alluding to the incompatibility of the two separate phase descriptions for the ordering in Pt-Al and Pt-Cr, confirmed this.

Table 3.1. Excerpt from Pt-Al-Cr database with the ordered Pt-Al phases (L12) and Pt-Cr phases (PT3CR_L12) shown as separate composition sets.

```
$ THIS PHASE HAS A DISORDERED CONTRIBUTION FROM FCC_A1
TYPE_DEFINITION & GES AMEND_PHASE_DESCRIPTION L12 DIS_PART FCC_A1,,,!
TYPE_DEFINITION ( GES AMEND_PHASE_DESCRIPTION L12 MAJ 1 PT:PT:PT:PT:VA!
TYPE_DEFINITION ( GES AMEND_PHASE_DESCRIPTION L12 C-S ,, AL:AL:AL:PT:VA!
TYPE_DEFINITION ( GES AMEND_PHASE_DESCRIPTION L12 C-S ,, AL:AL:PT:PT:VA!
TYPE_DEFINITION ( GES AMEND_PHASE_DESCRIPTION L12 C-S ,, AL:PT:PT:PT:VA!
PHASE L12  %&(  5 .25   .25   .25   .25  1 !
    CONSTITUENT L12  :AL,PT : AL,PT : AL,PT : AL,PT : VA : !

$ THIS PHASE HAS A DISORDERED CONTRIBUTION FROM FCC_A1
TYPE_DEFINITION F GES AMEND_PHASE_DESCRIPTION PT3CR_L12 DIS_PART FCC_A1,,,!
TYPE_DEFINITION G GES AMEND_PHASE_DESCRIPTION PT3CR_L12 MAJ 1 PT:PT:PT:PT:VA:!
TYPE_DEFINITION G GES AMEND_PHASE_DESCRIPTION PT3CR_L12 C-S ,, CR:CR:CR:PT:VA:!
TYPE_DEFINITION G GES AMEND_PHASE_DESCRIPTION PT3CR_L12 C-S ,, CR:CR:PT:PT:VA:!
TYPE_DEFINITION G GES AMEND_PHASE_DESCRIPTION PT3CR_L12 C-S ,, CR:PT:PT:PT:VA:!
PHASE PT3CR_L12 FG  5 .25   .25   .25   .25   1 !
    CONSTITUENT PT3CR_L12  :CR,PT : CR,PT : CR,PT : CR,PT : VA :  !
```

The database therefore had to be changed. The ordered fcc phases in the Pt-Cr and Pt-Al systems were described in one 4SL-CEF set and all possible permutations of species on the sublattices were included (Table 3.2). This could only be done by adding 700+ parameters to the database as well, as well as several functions. Many of the values could be grouped together assuming identical Gibbs energies for composition sets with identical ratios of elements. For simplification, only 0-degree interaction parameters (L values) were assigned variables, while the 1-degree L values were set to zero. Lastly, for completion of the 4SL-CEF model for the ternary system, the functions for ordered fcc phases in the Al-Cr were defined. However, these values were set to zero because these phases (CrAl and Cr_3Al) are not experimentally encountered in the binary, nor are they stabilised by Pt, except T3≈$CrAl_3$, a phase that is not observed in the Cr-Al binary diagram but listed in Pearson's Handbook as a probable AuCu-type ordered phase.

Table 3.2. Excerpt from Pt-Al-Cr database with the ordered Pt-Al phases and Pt-Cr phases shown as a single composition set (L12).

```
TYPE_DEFINITION ) GES AMEND_PHASE_DESCRIPTION L12 DIS_PART FCC_A1,,,!
$ THIS PHASE HAS A DISORDERED CONTRIBUTION FROM FCC_A1
TYPE_DEFINITION & GES AMEND_PHASE_DESCRIPTION L12 MAJ 1 PT:PT:PT:PT:VA:!
TYPE_DEFINITION ( GES AMEND_PHASE_DESCRIPTION L12 C-S ,, PT:PT:PT:AL:VA:!
TYPE_DEFINITION ( GES AMEND_PHASE_DESCRIPTION L12 C-S ,, PT:PT:AL:PT:VA:!
TYPE_DEFINITION ( GES AMEND_PHASE_DESCRIPTION L12 C-S ,, PT:AL:PT:PT:VA:!
TYPE_DEFINITION ( GES AMEND_PHASE_DESCRIPTION L12 C-S ,, AL:PT:PT:PT:VA:!
TYPE_DEFINITION ( GES AMEND_PHASE_DESCRIPTION L12 C-S ,, AL:AL:AL:PT:VA:!
TYPE_DEFINITION ( GES AMEND_PHASE_DESCRIPTION L12 C-S ,, AL:AL:PT:AL:VA:!
TYPE_DEFINITION ( GES AMEND_PHASE_DESCRIPTION L12 C-S ,, AL:PT:AL:AL:VA:!
TYPE_DEFINITION ( GES AMEND_PHASE_DESCRIPTION L12 C-S ,, PT:AL:AL:AL:VA:!
TYPE_DEFINITION ( GES AMEND_PHASE_DESCRIPTION L12 C-S ,, AL:AL:PT:PT:VA:!
TYPE_DEFINITION ( GES AMEND_PHASE_DESCRIPTION L12 C-S ,, AL:PT:PT:AL:VA:!
TYPE_DEFINITION ( GES AMEND_PHASE_DESCRIPTION L12 C-S ,, PT:AL:PT:AL:VA:!
TYPE_DEFINITION ( GES AMEND_PHASE_DESCRIPTION L12 C-S ,, AL:PT:AL:PT:VA:!
TYPE_DEFINITION ( GES AMEND_PHASE_DESCRIPTION L12 C-S ,, PT:AL:AL:PT:VA:!
TYPE_DEFINITION ( GES AMEND_PHASE_DESCRIPTION L12 C-S ,, PT:PT:AL:AL:VA:!
TYPE_DEFINITION ( GES AMEND_PHASE_DESCRIPTION L12 C-S ,, PT:PT:PT:CR:VA:!
TYPE_DEFINITION ( GES AMEND_PHASE_DESCRIPTION L12 C-S ,, PT:PT:CR:PT:VA:!
TYPE_DEFINITION ( GES AMEND_PHASE_DESCRIPTION L12 C-S ,, PT:CR:PT:PT:VA:!
TYPE_DEFINITION ( GES AMEND_PHASE_DESCRIPTION L12 C-S ,, CR:PT:PT:PT:VA:!
TYPE_DEFINITION ( GES AMEND_PHASE_DESCRIPTION L12 C-S ,, CR:CR:CR:PT:VA:!
TYPE_DEFINITION ( GES AMEND_PHASE_DESCRIPTION L12 C-S ,, CR:CR:PT:CR:VA:!
TYPE_DEFINITION ( GES AMEND_PHASE_DESCRIPTION L12 C-S ,, CR:PT:CR:CR:VA:!
TYPE_DEFINITION ( GES AMEND_PHASE_DESCRIPTION L12 C-S ,, PT:CR:CR:CR:VA:!
TYPE_DEFINITION ( GES AMEND_PHASE_DESCRIPTION L12 C-S ,, CR:CR:PT:PT:VA:!
TYPE_DEFINITION ( GES AMEND_PHASE_DESCRIPTION L12 C-S ,, CR:PT:PT:CR:VA:!
TYPE_DEFINITION ( GES AMEND_PHASE_DESCRIPTION L12 C-S ,, PT:CR:PT:CR:VA:!
TYPE_DEFINITION ( GES AMEND_PHASE_DESCRIPTION L12 C-S ,, CR:PT:CR:PT:VA:!
TYPE_DEFINITION ( GES AMEND_PHASE_DESCRIPTION L12 C-S ,, PT:CR:CR:PT:VA:!
TYPE_DEFINITION ( GES AMEND_PHASE_DESCRIPTION L12 C-S ,, PT:PT:CR:CR:VA:!

PHASE L12  %)&( 5 .25   .25  .25   .25  1 !
CONSTITUENT L12 :AL,CR,PT%:AL,CR,PT%:AL,CR,PT%:AL%,CR,PT:VA:  !
```

Using several starting points for the calculations, the best extrapolation at 1000°C that was obtained can be seen in Figure 3.8.

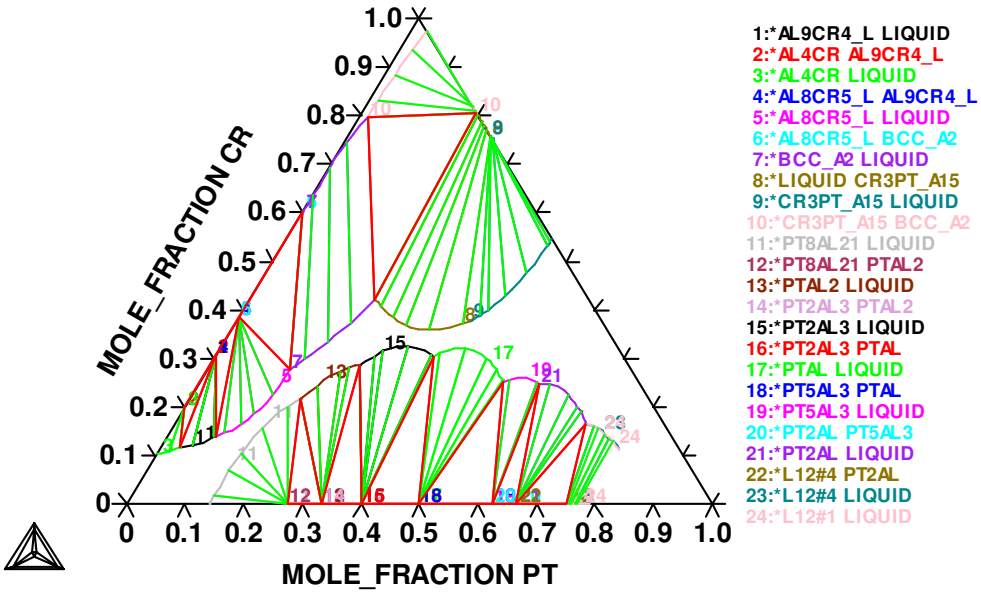

Figure 3.7. Extrapolation of Pt-Al, Cr-Pt and Al-Cr binary databases at 1000°C (with the ordered Pt-Al phases (L12) and Pt-Cr phases (PT3CR_L12) as separate composition sets).

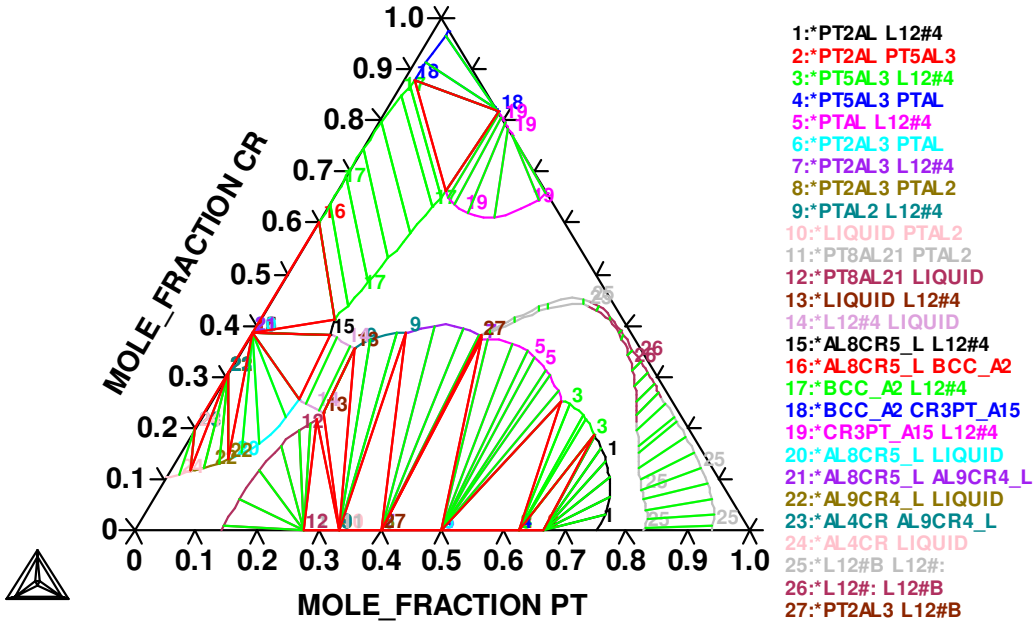

Figure 3.8. Extrapolation of Pt-Al, Cr-Pt and Al-Cr binary databases at 1000°C (with the ordered Pt-Al and Pt-Cr phases as a single composition set).

This was a much better extrapolation, and it was encouraging to see Pt_3Al finally appearing with significant phase stability (L12#4). The (Pt)/Pt_3Al phase region was also realised, as well as the (Cr)/Cr_3Pt/CrPt three-phase region (BCC_A2/CR3PT_A15/L12). The liquid phase was also now limited to the Al corner, which was more realistic.

4.4.2 The addition of ternary phase T1

Although Figure 3.8 was encouraging, it still was not good. The L12 phase field was much too stable (the large white area in the diagram). This would probably be resolved by the introduction of the ternary phase T1 ~Pt_3Al_2Cr with ~36-41 at.% Pt, 46-59 at.% Al; 18-2 at.% Cr. It was hoped that the inclusion of T1 would allow the experimentally identified equilibria between (Cr) [BCC_A2] and some of the Pt-Al intermetallic compounds like PTAL2, PT2AL3 and PTAL.

The model for T1 (designated TAO_1) was kept as simple as possible. It was modelled with three sublattices, with Pt atoms on the first, Al on the second and Cr on the third. It was also modelled as a stoichiometric compound, and a average composition of Pt_{50}:Al_{32}:Cr_{18} was used. Its parameters in the database are shown in Table 3.3.

Table 3.3. Excerpt from Pt-Al-Cr database showing how ternary phase T1 (TAO_1) was modelled.

```
PHASE TAO_1  %  3 .5  .32  .18  !
    CONSTITUENT TAO_1  :PT : AL : CR : !

   PARAMETER G(TAO_1,PT:AL:CR;0)  298.15  V01+V02*T+.5*GHSERPT+
.32*GHSERAL+.18*GHSERCR;   3000   N REF0 !
```

Without having to use the Thermo-Calc module PARROT which needs a so-called POP-file with experimental inputs, the values for V01 and V02 in Table 3.3 had to be guessed in order to make the calculation of the phase diagram. In order to make a calculated guess, the following procedure was followed:

- The melting point was calculated at the given composition using the database that did not include TAO_1. This was found to be in the order of ~1350°C.
- The Gibbs Energy for the liquid G_L was calculated at a temperature higher than the calculated melting point. 1400°C was used. At this temperature and composition, the

system would probably be liquid and TAO_1 would not have formed (which, from the experimental work and derived liquidus surface, is believed to melt congruently). It was calculated that G_L=-152 045 J/mol.

- The meaning of the parameter in Table 3.3 is actually the total Gibbs Energy for TAO_1
  $G_{TAO\_1(TOTAL)}=G_{TAO\_1(FORMATION)}$+0.5*GHSERPT+0.32*GHSERAL+0.18*GHSERCR
  where $G_{TAO\_1(FORMATION)}$ = V01+V02*T.
- By equating G_L and G_{TAO_1} at 1400°C, the estimated melting point of the system, one could calculate the Energy of Formation for TAO_1, $G_{TAO\_1(FORMATION)}$, i.e.
  $G_L= G_{TAO\_1(TOTAL)}= G_{TAO\_1(FORMATION)}$+0.5*GHSERPT+.32*GHSERAL+.18*GHSERCR
  Therefore:
  $G_{TAO\_1(FORMATION)}= G_L$-0.5*GHSERPT-.32*GHSERAL-.18*GHSERCR
- Calculated using Thermo-Calc, at 1400°C, the following values were obtained:
  GHSERPT=-111422 J/mol GHSERAL=-89847.2 J/mol GHSERCR=-81058.3 J/mol
- Therefore:
  $G_{TAO\_1(FORMATION)}$=-52992.4= V01+V02*T
  where T is in degrees Kelvin and is per definition T=1400°C+273=1673K
- Therefore:
  -52992.4= V01+V02*1673.
- By choosing a value for V01 one could then calculate a corresponding value for V02 at 1400°C. By using values for V01 between -130000 and -60000, V02 varied between 46.03 (huge temperature dependence) and 4.19 (much smaller temperature dependence). The corresponding value sets were input to the database, and the isothermal section for Pt-Al-Cr calculated at 1000°C and 600°C in order to compare them with the experimentally determined diagrams.

The experimentally determined isothermal sections at 600°C and 1000°C from Figures 2.193 and 2.247 are shown again in Figure 3.9 (a) and (b) for easy reference. The most satisfactory 1000°C isothermal section were obtained using V01= -120000 and V02=40.053 (Figure 3.10), while the most satisfactory 600°C isothermal section were obtained using V01= -100000 and V02=28.098 (Figure 3.11). A liquidus surface projection was calculated

as well, using the values for V01 and V02 that had been used for the 1000°C calculation (Figure 3.12 (a)).

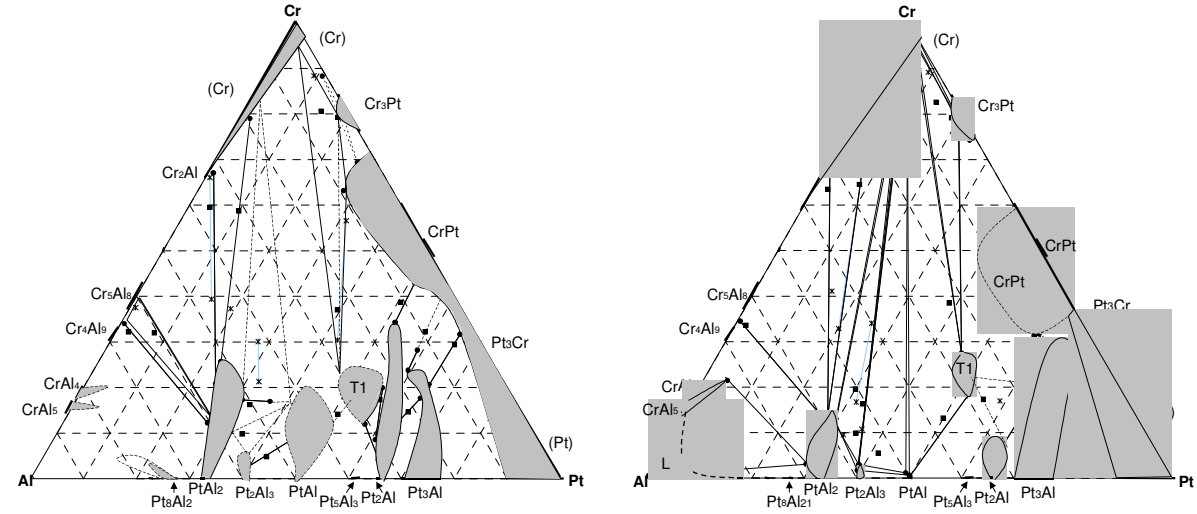

(a) (b)

Figure 3.9. Experimentally determined isothermal sections at (a) 600°C and (b) 1000°C for Pt-Al-Cr.

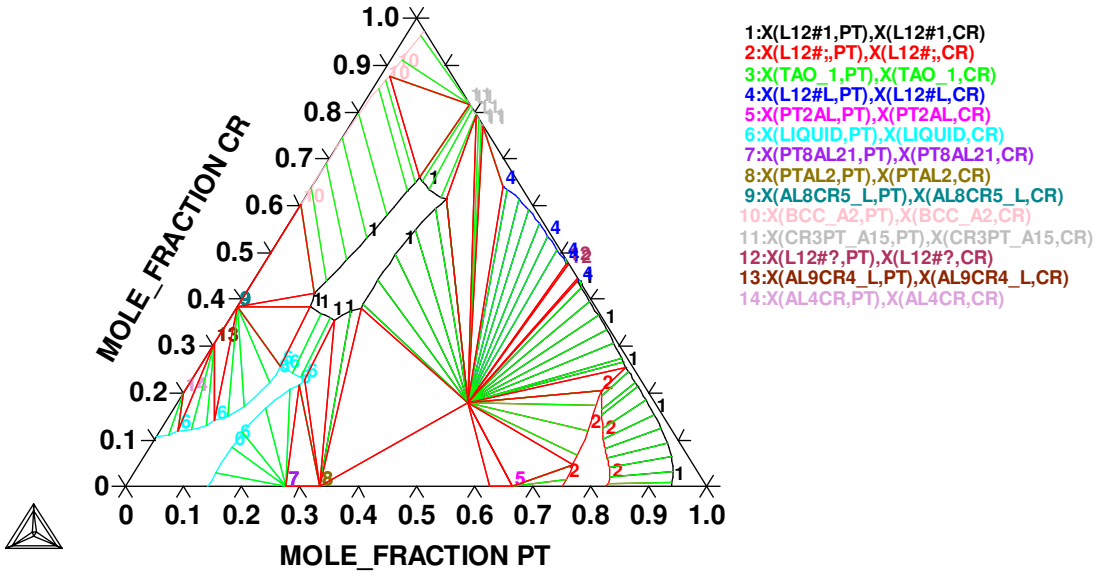

Figure 3.10. Best extrapolation of Pt-Al, Cr-Pt and Al-Cr binary databases at 1000°C with ternary phase T1 added.

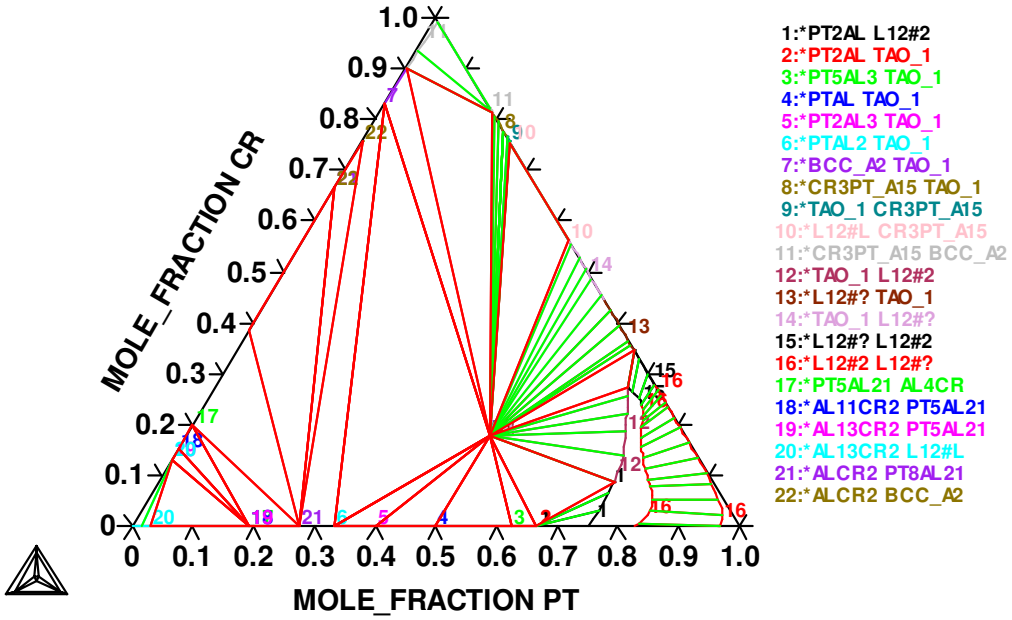

Figure 3.11. Best extrapolation of Pt-Al, Cr-Pt and Al-Cr binary databases at 600℃ with ternary phase T1 added.

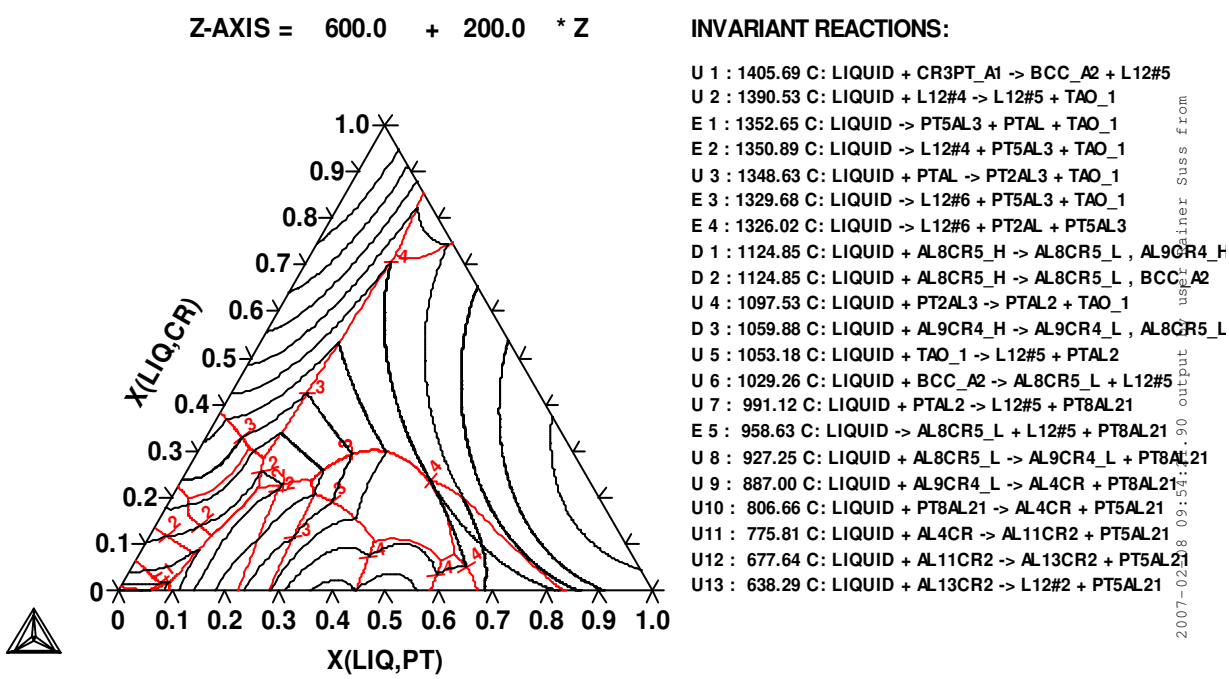

(a)

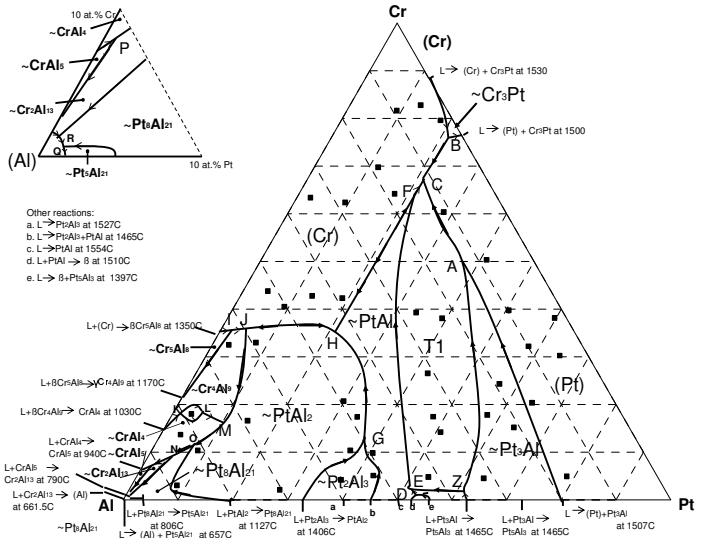

(b)

Figure 3.12. Comparison of Pt-Al-Cr liquidus surface projections: a) Calculation (using an extrapolation of Pt-Al, Cr-Pt and Al-Cr binary databases with ternary phase T1 added.); b) Experimental (this work).

It was good to see that T1 could be modelled as a stable phase. It was very good to see the following three-phase fields appearing in accordance with the experimental diagrams:

- At 600°C:
  - (Cr) + Cr_3Pt + T1
  - Cr_3Pt + CrPt + T1
- At 1000°C:
  - Pt_2Al + Pt_3Al + T1.

Many of the modelled equilibria coincided with the experimental results, albeit as part of three-phase equilibria. Both models showed the Pt_3Al/(Pt) equilibria. The Pt_3Al phase field decreased in size and looked more realistic, while the stable L12 phase field that cut across the diagram in Figure 3.7 has significantly decreased.

With regards to the liquidus surface: Some of the calculated phase surfaces were in very good agreement with the experimentally determined ones, e.g. (Cr), ~Cr_3Pt and (Al), while others were quite close (~Cr_5Al_8, ~Cr_4Al_9, ~$CrAl_4$, ~$CrAl_5$ (~Cr_2Al_{11}) and ~Cr_2Al_{13}). Those

calculated surfaces that really stood out as being incorrect were ~$PtAl_2$, ~PtAl, T1 and the ordered (~Pt_3Al) and disordered ((Pt)) fcc phases.

In general, the results, especially at 600°, were very encouraging. Although there were many obvious problems, it was believed that most of these would be rectified in time because:

- Except for adding the ternary phase and modelling the ordered fcc phases the same, this effort was not much more than an extrapolation of the binaries.
- Many values in the database have been set to zero for simplification.
- Only a few variables in the database were selected for optimisation thus far, and these have been "optimised" manually and not with Thermo-Calc's Parrot module.
- No POP-file with the experimental data for Pt-Al-Cr has been prepared yet (these can include phase compositions in equilibrium with each other at known temperatures, reaction information, enthalpies, etc.). Thermo-Calc uses the information in the POP-file and, through iteration, calculates the parameters required (those that were set to be changed) to best fit the data in the POP-file.
- Finally, no ternary interaction parameters (L values) for mixing on the sublattices for the Pt-Al intermetallics have been introduced yet to enable extension into the ternary.

The latter aspect was believed to be the single most important matter that had to be addressed in order to improve the model.

4.4.3 Optimisation: The evolution of the model parameters

The optimisation was done using a newer version of the software, Thermo-Calc Classic Version R (TCC-R). Repeating the work above with the new version was problematic at first, because the POLY module (responsible for the equilibrium calculations) in TCC-R can only accept up to 9 composition sets for a specific phase, whereas before the number was unlimited. In the database file (TDB file) used thus far, 28 type definitions (TYPE_DEFs) for additional composition sets of the $L1_2$ ordered phase were used. These had to be reduced. In principle one would not need to add any composition set to a solution phase, because the new Global Minimization Technique implemented in TCC-R will first try to detect all possibly required additional composition sets prior to calculating the final equilibrium state. However, not adding any composition sets was unsuccessful. Using the TYPE_DEF for

PT:PT:PT:PT:VA (Pt) as the major constituents for L12, and adding PT:PT:PT:AL:VA, PT:PT:PT:CR:VA and CR:CR:PT:PT:VA as additional composition sets for the phases Pt_3Cr, Pt_3Al and CrPt) yielded good results.

4.4.3.1 Extending Pt_2Al only

It was initially decided to add extension of the Pt-Al intermetallics on a one-by-one basis in order to limit the amount of variables to optimise for the different parameters. It was decided to start with the Pt-rich side, and Pt_2Al was the first phase chosen to be optimised.

At this stage, Pt_2Al was modelled as shown in Table 3.4.

Table 3.4. Excerpt from Pt-Al-Cr database showing how ternary phase Pt_2Al was initially modelled.

```
PHASE PT2AL  %  2 .334   .666 !
    CONSTITUENT PT2AL  :AL : PT :  !

   PARAMETER G(PT2AL,AL:PT;0)  298.15  -84989+24.9*T+.334*GHSERAL#
  +.666*GHSERPT#;   3000   N REF0 !
```

The initial model (Table 3.4) means it was modelled with 2 sublattices, with Al on the first and Pt on the second. One would introduce Cr by replacing or adding to the constituents of one or both sublattices. The experimental phase diagrams showed substitution on both sublattices, but with very little extension at 1000°C (Figure 4.9). Cr was introduced by adding the parameters shown in Table 3.5.

Table 3.5. Excerpt from Pt-Al-Cr database showing how ternary phase Pt_2Al was modelled with the introduction of interaction parameters.

```
PHASE PT2AL  %  2 .334   .666 !
    CONSTITUENT PT2AL  :AL,CR : PT,CR :  !
PARAMETER G(PT2AL,AL:CR;0)  298.15 V01+0.334*GHSERAL#+0.666*GHSERCR#;
3000   N REF0 !
PARAMETER G(PT2AL,CR:PT;0)  298.15  V02+0.334*GHSERCR#+.666*GHSERPT#;
3000   N REF0 !
PARAMETER G(PT2AL,CR:CR;0)  298.15  V03+GHSERCR#;   3000   N REF0 !
PARAMETER G(PT2AL,AL,CR:PT;0)  298.15  V04;   3000   N REF0 !
PARAMETER G(PT2AL,AL:PT,CR;0)  298.15  V05;   3000   N REF0 !
```

In an attempt to minimise the amount of variables to be optimised:

- two more possible interaction parameters, `G(PT2AL,AL,CR:CR;0)` and `G(PT2AL,CR:PT,CR;0)`, were initially not included. It was felt that the total absence of either Pt or Al from any sublattice was unlikely;
- mixing of Cr with another constituent was only allowed on one of either sublattices but not both;
- only 0-degree interaction parameters were assigned variables; and
- none of the variables were given a temperature dependent term.

The absolute values that were assigned to the variables were initially totally random. The signs of the values (negative or positive) were not. The following values were assigned at first:

```
V01=-5000; V02=-5000; V03=5000; V04=-50000; V05=-50000.
```

V04 and V05 were made highly negative compared to V01 and V02 in attempt to make the mixing of Al and Cr and that of Pt and Cr stable. A positive value was assigned to V03 to make Pt_2Al consisting of only Cr (which would in effect be bcc) unstable.

Figure 3.13 shows the calculated isothermal section at 1000°C using these values. It was identical to the one calculated before (Figure 3.10) except that Pt_2Al extended with almost 10 at.% Cr into the ternary. This was encouraging. It was interesting to note that it was extending in the direction towards a metastable composition Pt_2Cr which suggested that variable V02 for `G(PT2AL,CR:PT;0)` had to be more positive in order to make "Pt_2Cr" less stable.

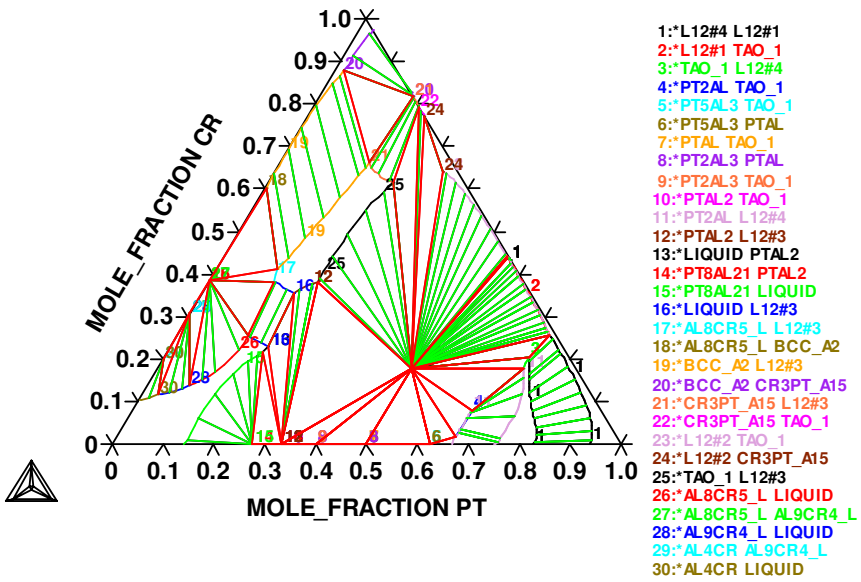

Figure 3.13. First calculated 1000°C isothermal section for Pt-Al-Cr with extending Pt_2Al.

Subsequently, several calculations were made varying the values for variables V01 to V05 in an attempt to increase the extension of Pt_2Al, change the direction of extension and possibly giving it a homogeneity range, without adversely affecting the stability of any of the surrounding phases, particularly Pt_3Al (L12) and T1 (TAO_1).

The Pt-rich corner of a calculated 1000°C isothermal section is shown in Figure 3.14. The following values were used:

```
V01=20000; V02=50000; V03=500; V04=-90000; V05=-124900.
```

It can be seen that Pt_2Al was extending in a different direction, and that it had a ~2 at.% stability range. The values given above resulted in the diagram having the best attributes thus far. Values between 0 and 50000 for V01 - V03 did not seem to have a significant effect on the calculation. Values of 150000+ for both V04 and V05 significantly reduced the extension of Pt_3Al (L12). A value closer to 100000 for V04 and between 100000 and 150000 for V05 was better, with a value of 150000+ for V05 resulting in Pt_2Al extending through and beyond T1 (TAO_1) which was highly unrealistic.

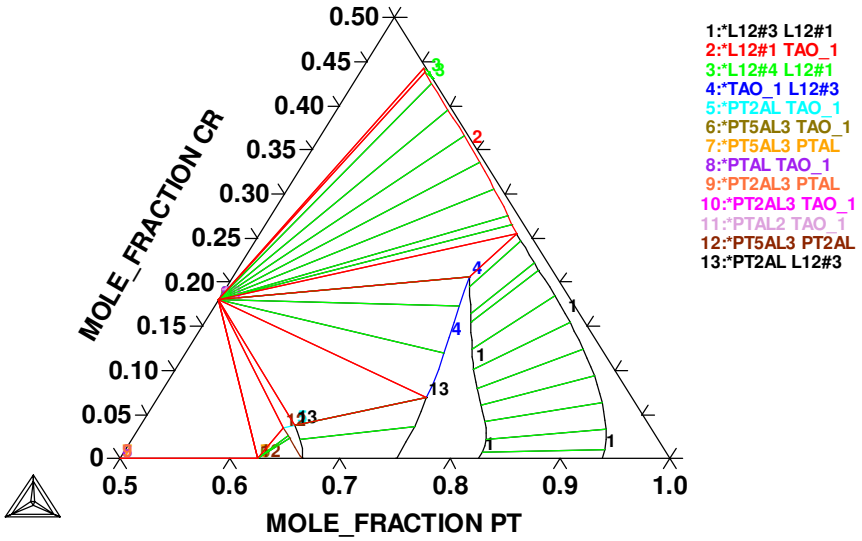

Figure 3.14. Calculated 1000°C isothermal section for Pt-Al-Cr with Pt_2Al extending ~4 at.% Cr and having stability range (phase width).

Although progress was made, the diagram was still not good. Furthermore, there were still inconsistencies between the 600°C and 1000°C isothermal sections, which implied that some of the variables needed the introduction of temperature dependency.

The initial enthalpy and entropy terms used were determined by:

$V04 = H_1 - T*S_1$
$-90000 = H_1 - (1273)*S_1$
$-100000 = H_1 - (873)*S_1$
(−100000 was arbitrarily chosen to be more negative at 600°C than at 1000°C)
$\therefore H_1 = -121825$
$\therefore S_1 = -25$
$\therefore$ **V04 = −121825+25*T**

$V05 = H_2 - T*S_2$
$-124900 = H_2 - (1273)*S_2$
$-140000 = H_2 - (873)*S_2$
(−140000 was arbitrarily chosen to be more negative at 600°C than at 1000°C)
$\therefore H_2 = -173019$
$\therefore S_2 = -37.8$
$\therefore$ **V05 = −173019+37.8*T**

Calculations with these values yielded similar results to before, and the best isothermal sections (not shown because of their similarity to Figure 3.15) were calculated after slight adjustments to V04 and V05,

V04 = −118000+19.9*T

V05 = −178000+44.7*T

The introduction of the temperature dependent terms insured similar behaviour of the system at both 600°C and 1000°C. However, it had reverted the direction of extension of Pt_2Al to what it used to be before (Figure 3.13), and its stability range had also disappeared.

In an attempt to rectify this problem, parameters `G(PT2AL,AL,CR:CR;0)` and `G(PT2AL,CR:PT,CR;0)` were added. To keep the model simple, identical values were used for the interaction parameters for Al and Cr mixing on the one sublattice, and for Pt and Cr on the other. After several calculations it was realised that it was also necessary to adjust V03 to a much higher positive value to avoid strange behaviour of the Pt_2Al phase. The results are shown in Figure 3.15. The model used for Pt_2Al is shown in Table 3.6.

Table 3.6. Excerpt from Pt-Al-Cr database showing the Pt_2Al model after further optimisation.

```
PHASE PT2AL  %  2 .334   .666 !

    CONSTITUENT PT2AL  :AL,CR : PT,CR :  !
PARAMETER G(PT2AL,AL:CR;0)  298.15  20000+0.334*GHSERAL#+0.666*GHSERCR#;
   3000   N REF0 !
PARAMETER G(PT2AL,CR:PT;0)  298.15  50000+0.334*GHSERCR#+.666*GHSERPT#;
   3000   N REF0 !
PARAMETER G(PT2AL,CR:CR;0)  298.15  150000+GHSERCR#;   3000   N REF0 !

PARAMETER G(PT2AL,AL:PT;0)  298.15  -84989+24.9*T+.334*GHSERAL#
  +.666*GHSERPT#;   3000   N REF0 !
PARAMETER G(PT2AL,AL,CR:PT;0)  298.15  -118000+19.9*T;   3000   N REF0 !
PARAMETER G(PT2AL,AL:PT,CR;0)  298.15  -178000+44.7*T;   3000   N REF0 !
PARAMETER G(PT2AL,AL,CR:CR;0)  298.15  -118000+19.9*T;   3000   N REF0 !
PARAMETER G(PT2AL,CR:PT,CR;0)  298.15  -178000+44.7*T;   3000   N REF0 !
```

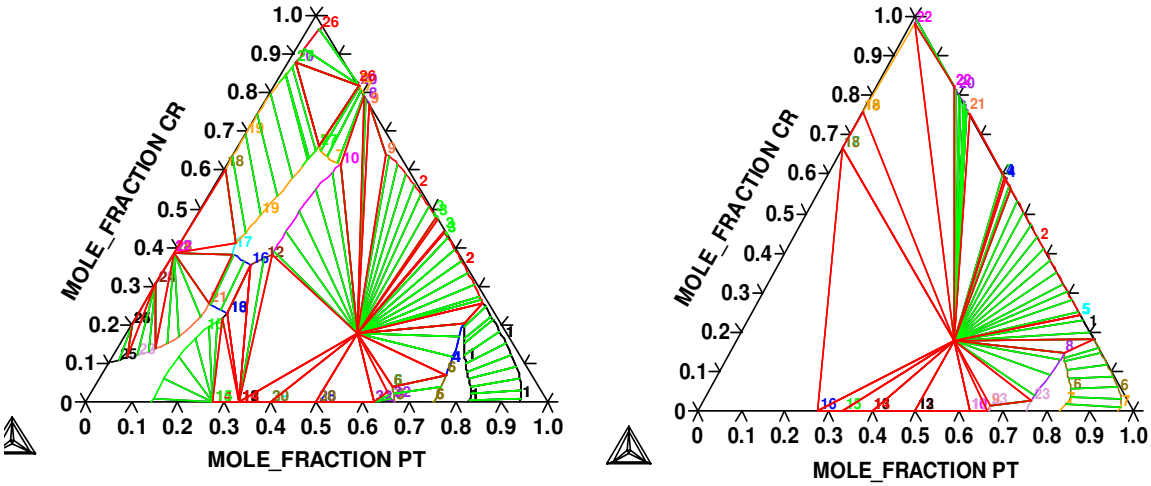

Figure 3.15. Calculated 600℃ and 1000℃ isothermal sections for Pt-Al-Cr with temperature dependent terms for interaction parameters.

Although the model for Pt_2Al was now more complex and arguably more complete, not much had been achieved in comparison with the earlier results of Figures 4.10 and 4.11. Pt_2Al was extending somewhat into the ternary (~4 at.%), and did so for both assessed temperatures, but the rest of the diagrams had not improved.

By varying the values of the variables in a systematic manner it was also realised that the extension of Pt_2Al was hampered by the stability of T1 and not much could be done about it if the latter was included. Since the stability of Pt_2Al was dependent on that of T1, and since the stability of the other Pt-Al intermetallic compounds would most probably also depend on T1's stability and that of each other, it was decided to step away from the initial plan of optimising them on a one-by-one basis, but to rather include interaction parameters for all of them and optimising them together.

4.4.3.2 Extending Pt_2Al, PtAl and $PtAl_2$ simultaneously

Pt_2Al, PtAl and $PtAl_2$ were chosen for optimisation because they extended significantly into one or both of the experimental isothermal sections. Since Pt_2Al_3 did not, it was decided not to optimise it any further and keep it as a line compound. This also helped in minimising the number of optimising variables.

PtAl and $PtAl_2$ were modelled in similar fashion to Pt_2Al, and for a first approximation identical values were used for similar interactions, e.g.

```
G(PT2AL,AL,CR:PT;0) = G(PTAL,AL,CR:PT;0) = G(PTAL2,AL,CR:PT;0).
```

The first results with interaction parameters for all three compounds are shown in Figures 4.16 and 4.17.

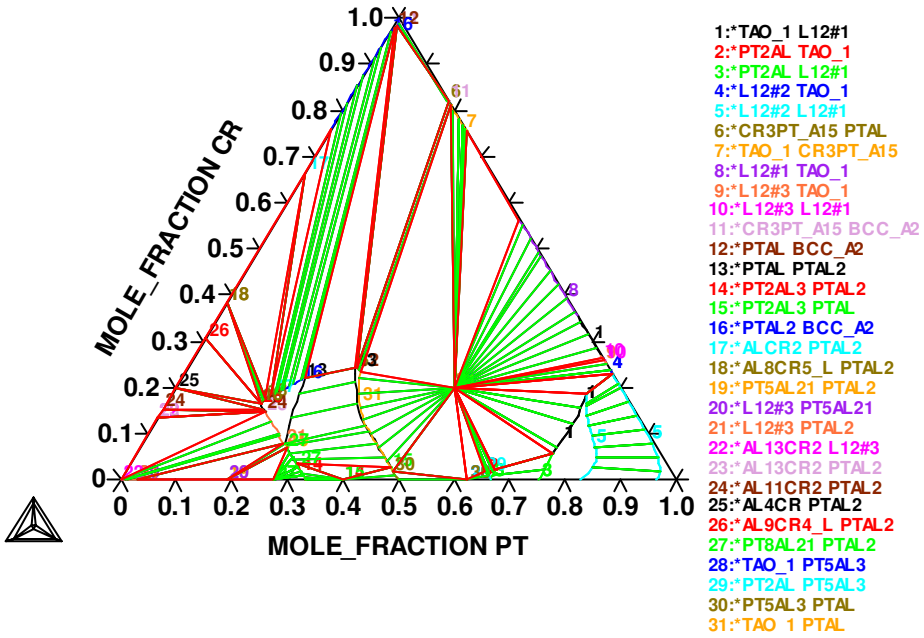

Figure 3.16. First calculated 600℃ isothermal section for Pt-Al-Cr with extending Pt_2Al, PtAl and $PtAl_2$.

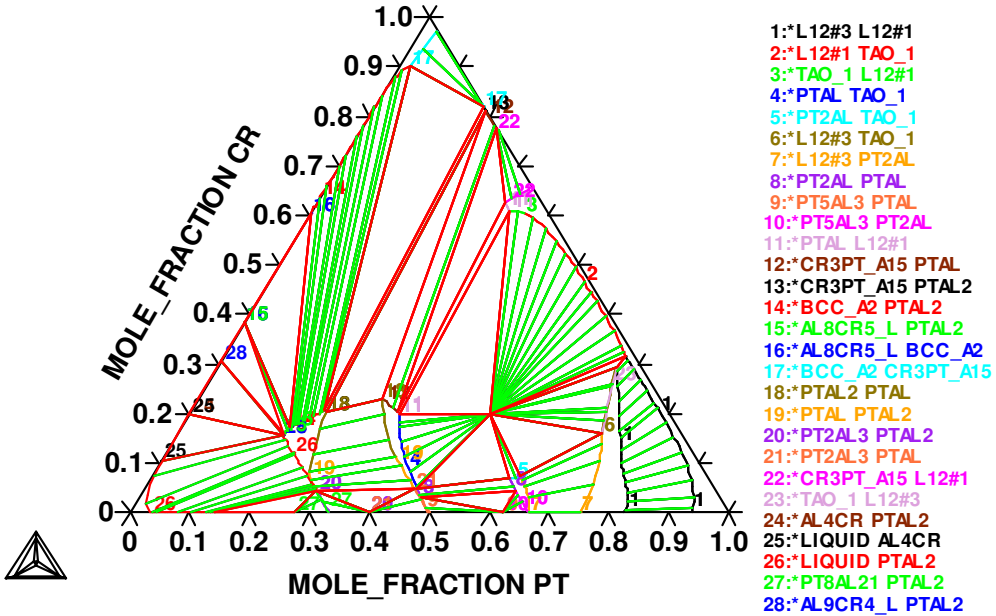

Figure 3.17. First calculated 1000℃ isothermal section for Pt-Al-Cr with extending Pt_2Al, PtAl and $PtAl_2$.

It was highly encouraging to see that not only did the three Pt-Al intermetallics extend into the ternary, but that many of the required equilibria were already correct and the stable L12 phase field in the centre of the diagram in Figure 3.10 had disappeared. $PtAl_2$ even had stability over a composition range at both temperatures, while PtAl and Pt_2Al had some at 600°C. Up to then, these two diagrams were the closest to the experimental ones, and proof that the optimisation process was on the right track. The biggest problems that needed to be rectified were a number of incorrect phase relations:

At 1000°C:

- BCC_A2 - CR3PT_A15 - PTAL2
- CR3PT_A15 - PTAL2 - PTAL
- CR3PT_A15 - L12 (CrPt) - PTAL
- L12 (CrPt) - PTAL - TAO_1
- CR3PT_A15 - PTAL
- PTAL2 - PT2AL3 - PTAL

At 600°C:

- BCC_A2 - PTAL - CR3PT_A15
- CR3PT_A15 - PTAL - PT2AL

After a lot of tweaking of optimising variables, a much better 1000°C isothermal section was achieved, but not at 600°C. The results based on the model parameters given in Table 3.7 are shown in Figure 3.18.

Table 3.7. Excerpt from Pt-Al-Cr database showing the parameters for Pt_2Al, PtAl, $PtAl_2$ and TAO_1 after further optimisation.

```
PHASE PT2AL  %  2 .334   .666 !
    CONSTITUENT PT2AL  :AL,CR : PT,CR :  !
 PARAMETER G(PT2AL,AL:CR;0)  298.15  20000+0.334*GHSERAL#+0.666*GHSERCR#;
   3000   N REF0 !
PARAMETER G(PT2AL,CR:PT;0)  298.15  50000+0.334*GHSERCR#+.666*GHSERPT#;
   3000   N REF0 !
PARAMETER G(PT2AL,CR:CR;0)  298.15  150000+GHSERCR#;   3000   N REF0 !

   PARAMETER G(PT2AL,AL:PT;0)  298.15  -84989+24.9*T+.334*GHSERAL#
  +.666*GHSERPT#;   3000   N REF0 !
PARAMETER G(PT2AL,AL,CR:PT;0)  298.15  -118000+19.9*T;   3000   N REF0 !
PARAMETER G(PT2AL,AL:PT,CR;0)  298.15  -178000+44.7*T;   3000   N REF0 !
PARAMETER G(PT2AL,AL,CR:CR;0)  298.15  -118000+19.9*T;   3000   N REF0 !
PARAMETER G(PT2AL,CR:PT,CR;0)  298.15  -178000+44.7*T;   3000   N REF0 !
```

Table 3.7. Excerpt from Pt-Al-Cr database showing the parameters for Pt_2Al, PtAl, $PtAl_2$ and TAO_1 after further optimisation (contd.).

```
PHASE PTAL  %  2 .5   .5 !
    CONSTITUENT PTAL  :AL,CR : PT,CR :  !

   PARAMETER G(PTAL,AL:PT;0)  298.15  -94071+24.1*T+.5*GHSERAL#
  +.5*GHSERPT#;   3000   N REF0 !
  PARAMETER G(PTAL,AL:CR;0)  298.15  20000+0.5*GHSERAL#+0.5*GHSERCR#;
3000   N REF0 !
PARAMETER G(PTAL,CR:PT;0)  298.15  50000+0.5*GHSERCR#+0.5*GHSERPT#;
3000   N REF0 !
PARAMETER G(PTAL,CR:CR;0)  298.15 250000+GHSERCR#;   3000   N REF0 !
PARAMETER G(PTAL,AL,CR:PT;0)  298.15  -128000+19.9*T;   3000   N REF0 !
PARAMETER G(PTAL,AL:PT,CR;0)  298.15  -188000+44.7*T;   3000   N REF0 !
PARAMETER G(PTAL,AL,CR:CR;0)  298.15  -128000+19.9*T;   3000   N REF0 !
PARAMETER G(PTAL,CR:PT,CR;0)  298.15  -188000+44.7*T;   3000   N REF0 !


 PHASE PTAL2  %  2 .666   .334 !
    CONSTITUENT PTAL2  :AL,CR : PT,CR :  !

   PARAMETER G(PTAL2,AL:PT;0)  298.15  -87898+23.3*T+.666*GHSERAL#
  +.334*GHSERPT#;   3000   N REF0 !
 PARAMETER G(PTAL2,AL:CR;0)  298.15  +20000+0.666*GHSERAL#+0.334*GHSERCR#;
3000   N REF0 !
PARAMETER G(PTAL2,CR:PT;0)  298.15  +50000+0.666*GHSERCR#+0.334*GHSERPT#;
3000   N REF0 !
PARAMETER G(PTAL2,CR:CR;0)  298.15  +170000+GHSERCR#;   3000   N REF0 !
PARAMETER G(PTAL2,AL,CR:CR;0)  298.15  -108000+19.9*T;   3000   N REF0 !
PARAMETER G(PTAL2,CR:PT,CR;0)  298.15  -168000+44.7*T;   3000   N REF0 !
PARAMETER G(PTAL2,AL,CR:PT;0)  298.15  -108000+19.9*T;   3000   N REF0 !
PARAMETER G(PTAL2,AL:PT,CR;0)  298.15  -168000+44.7*T;   3000   N REF0 !

PARAMETER G(TAO_1,PT:AL:CR;0)  298.15  -130000+40.28*T+.5*GHSERPT+
.3*GHSERAL+.2*GHSERCR; 3000 N REF0 !
```

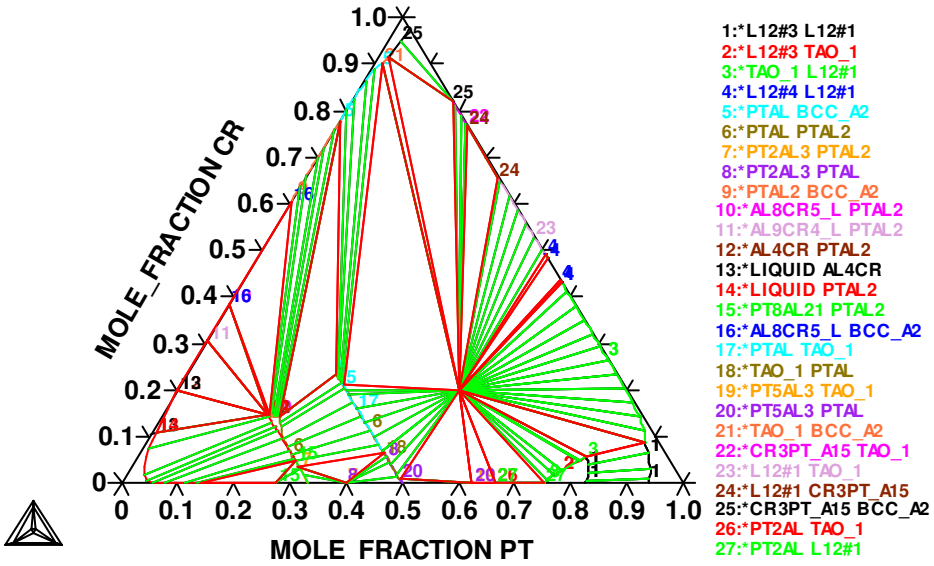

Figure 3.18. 1000°C isothermal section for Pt-Al-Cr after further optimisation of Pt_2Al, PtAl $PtAl_2$ and T1.

It was clear that the direction of extension for Pt_2Al, PtAl and $PtAl_2$ could not be changed. There was also no obvious way to get rid of the PTAL2 - PT2AL3 - PTAL equilibrium (this equilibrium was experimentally observed at 600°C but not at 1000°C). The other problematic equilibria that were mentioned before could only be improved by making T1 more stable, and that was done by making its enthalpy term more negative as can be seen in Table 3.7. Although these equilibria were now more realistic (BCC_A2 - PTAL - PT2AL, BCC_A2 - CR3PT_A15 - TAO_1, and CR3PT_A15 - L12 (CrPt) - TAO_1), Pt_3Al (L12) did not extend as much as before.

It was decided to give non-zero values to parameters in the L12 model comprising the functions `ALCR2PT`, `ALCRPT2` and `AL2CRPT`. For simplification, identical values for each function were used in the subsequent calculations. Negative values were initially used to make these energetically more favourable, but surprisingly only positive values yielded good results (as was the case for other functions for the L12 model, like `APL2FCC`, `UL0`, `UL1` and `REC2`). `FUNCTION ALCR2PT = FUNCTION ALCR2PT = FUNCTION ALCR2PT = 20 000` increased the extent of Pt_3Al (L12) at 1000°C while a value of 40 000 was better for calculations at 600°C. Similar to Pt_2Al before (Table 3.6), temperature dependency had to be introduced, and by simultaneously solving the equation G=H−T*S for both temperatures, it was determined that H=83650 and S=−50, i.e.

```
FUNCTION ALCR2PT = FUNCTION ALCR2PT = FUNCTION ALCR2PT = 83 650-50*T.
```

Using these values for calculations, most of the required equilibria were in order, the three Pt-Al compounds extended into the ternary and Pt_3Al (L12) extended into the ternary as before (Figures 4.19).

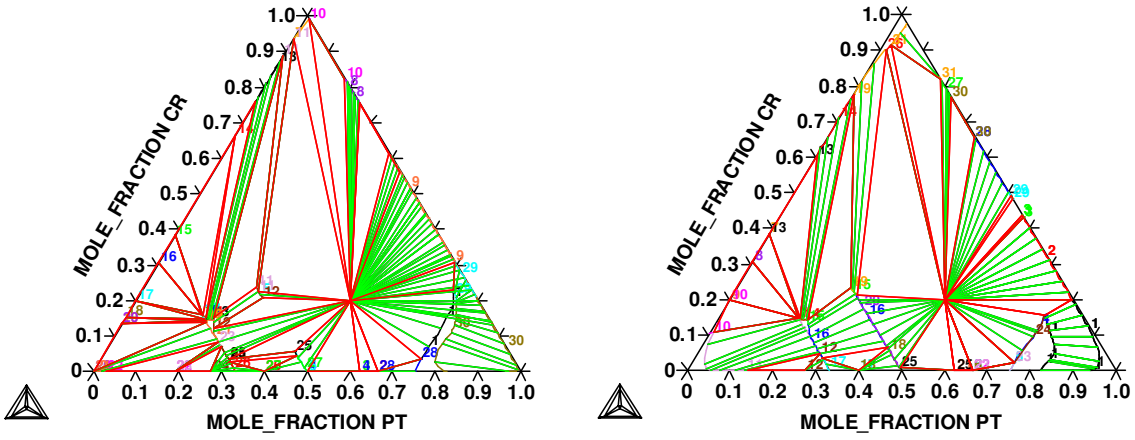

Figure 3.19. 1000 °C and 600 °C isothermal section for Pt-Al-Cr after further optimisation of L12.

However, $PtAl_2$ showed a strange discontinuity at 600°C. This problem was solved by making the phase more stable. This was achieved by making the parameters `G(PTAL,AL,CR:PT;0)`, `G(PTAL,AL:PT,CR;0)`, `G(PTAL,AL,CR:CR;0)` and `G(PTAL,CR:PT,CR;0)` more negative and decreasing `G(PTAL,CR:CR;0)` from 250000 to 200000 (Figure 3.20). PtAl also exhibited more phase width at both temperatures.

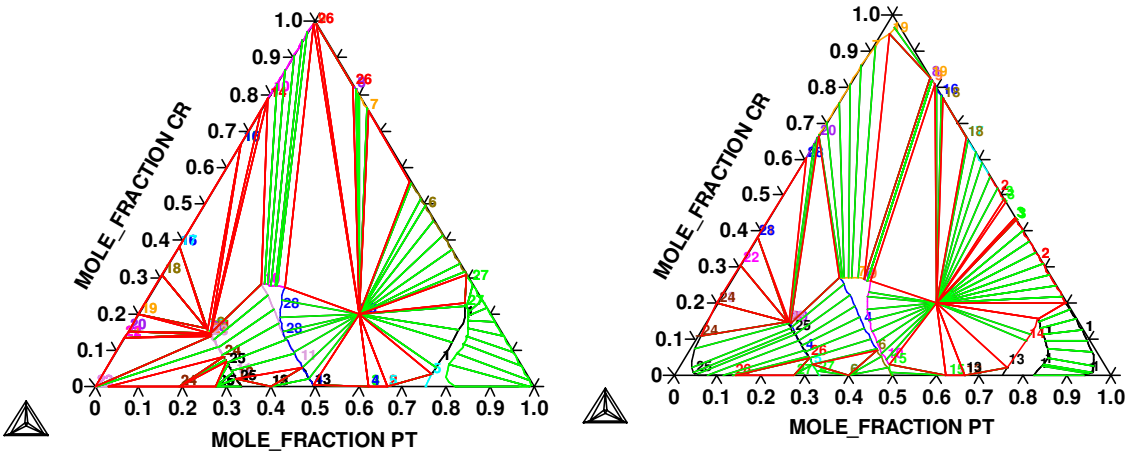

Figure 3.20. 1000 °C and 600 °C isothermal sections for Pt-Al-Cr after further optimisation of PtAl.

Unfortunately, the phase relations between PTAL, BCC_A2, PT2AL, CR3PT_A15 and L12 (CrPt) were all wrong again at 1000°C. These were fixed by varying the optimising variables for PtAl (making TAO_1 even more stable was unsuccessful and affected L12 severely) and doing several calculations at 600°C and 1000°C. Table 3.8 shows the best values at 1000°C and Table 3.9 the best values at 600°C.

Table 3.8. Excerpt from Pt-Al-Cr database showing the parameters for PtAl after further optimisation yielding good results at 1000 °C.

```
PARAMETER G(PTAL,AL,CR:PT;0)   298.15  -128000+19.9*T;    3000   N REF0 !
PARAMETER G(PTAL,AL:PT,CR;0)   298.15  -188000+44.7*T;    3000   N REF0 !
PARAMETER G(PTAL,AL,CR:CR;0)   298.15  -128000+19.9*T;    3000   N REF0 !
PARAMETER G(PTAL,CR:PT,CR;0)   298.15  -188000+44.7*T;    3000   N REF0 !
```

Table 3.9. Excerpt from Pt-Al-Cr database showing the parameters for PtAl after further optimisation yielding good results at 600℃.

```
PARAMETER G(PTAL,AL,CR:PT;0)   298.15  -147000+20*T;    3000   N REF0 !
PARAMETER G(PTAL,AL:PT,CR;0)   298.15  -203000+45*T;    3000   N REF0 !
PARAMETER G(PTAL,AL,CR:CR;0)   298.15  -147000+20*T;    3000   N REF0 !
PARAMETER G(PTAL,CR:PT,CR;0)   298.15  -203000+45*T;    3000   N REF0 !
```

By calculating the Gibbs Energy for each parameter at each temperature and then simultaneously solving the equation G=H−T*S for each parameter at both temperatures, new enthalpy and entropy values were determined for each parameter. For example:

$G(PTAL,AL,CR:PT;0)_{1273} = -128000+19.9*1273 = -103185$

$G(PTAL,AL,CR:PT;0)_{873} = -147000+20*873 = -129540$

$-103185 = H-(1273)*S$

$-129540 = H-(873)*S$

$\therefore H = -187060$

$\therefore S = 65.9$

$\therefore$ **G(PTAL,AL,CR:PT;0) = -187060+65.9*T**

The newly calculated values are shown in Table 3.10 with the improved calculated diagrams shown in Figure 3.21.

Table 3.10. Excerpt from Pt-Al-Cr database showing the parameters for PtAl after further optimisation yielding good results at both 600℃ and 1000℃.

```
PARAMETER G(PTAL,AL,CR:CR;0)   298.15  -187060+65.9*T;    3000   N REF0 !
PARAMETER G(PTAL,CR:PT,CR;0)   298.15  -234908+81.6*T;    3000   N REF0 !
PARAMETER G(PTAL,AL,CR:PT;0)   298.15  -187060+65.9*T;    3000   N REF0 !
PARAMETER G(PTAL,AL:PT,CR;0)   298.15  -234908+81.6*T;    3000   N REF0 !
```

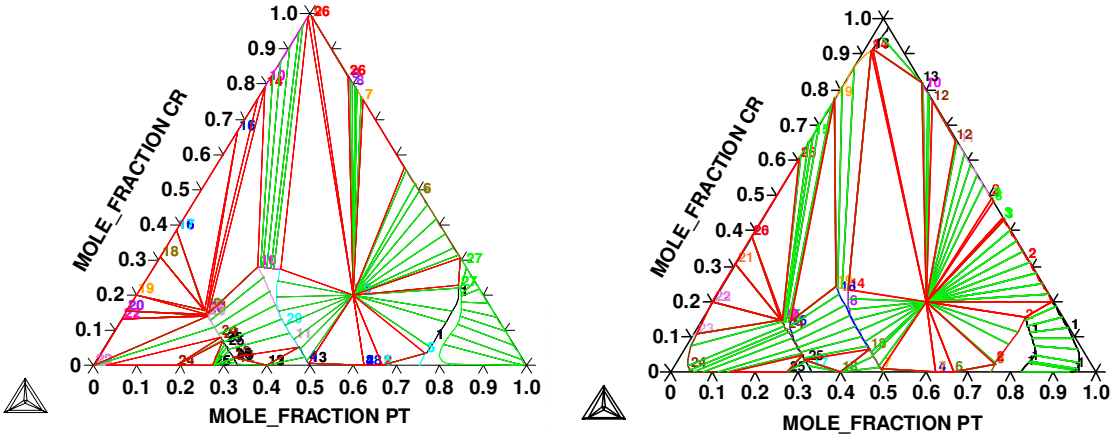

Figure 3.21. 1000℃ and 600℃ isothermal sections for Pt-Al-Cr after further optimisation of PtAl.

It was felt that the extension of Pt_3Al (L12) at 600°C was slightly too much compared to that at 1000°C. Therefore functions `ALCR2PT`, `ALCR2PT` and `ALCR2PT` were slightly adjusted to

```
FUNCTION ALCR2PT = FUNCTION ALCR2PT = FUNCTION ALCR2PT = 83 650-55*T.
```

An attempt was also made to extend Pt_2Al further, and the best results were achieved by using the values as shown in Table 3.11 compared to values of 20000 and 50000 for `G(PT2AL,AL:CR;0)-0.334*GHSERAL#-0.666*GHSERCR#` and `G(PT2AL,CR:PT;0)-0.334*GHSERCR#-0.666*GHSERPT#` respectively in Table 3.7.

Table 3.11. Excerpt from Pt-Al-Cr database showing tweaked parameters for Pt_2Al.

```
PHASE PT2AL  %  2 .334   .666 !
    CONSTITUENT PT2AL  :AL,CR : PT,CR :  !
 PARAMETER G(PT2AL,AL:CR;0)  298.15  10000+0.334*GHSERAL#+0.666*GHSERCR#;
   3000   N REF0 !
PARAMETER G(PT2AL,CR:PT;0)  298.15  20000+0.334*GHSERCR#+.666*GHSERPT#;
   3000   N REF0 !
```

Lastly, an attempt was made to give $PtAl_2$ a phase stability range similar to that of PtAl. This was achieved adjusting `G(PTAL2,CR:PT;0)` by varying the Gibbs energy of formation term only and doing calculations at both 600°C and 1000°C until satisfactory isothermal sections were calculated. Temperature dependency were introduced by calculating the Gibbs Energy for the parameter at each temperature and then simultaneously solving the equation G=H−T*S for both temperatures, thereby determining an enthalpy and entropy term (Table 3.12), compared to a value of 50000 for `G(PTAL2,CR:PT;0)-0.666*GHSERCR#-0.334*GHSERPT#` in Table 3.7.

Table 3.12. Excerpt from Pt-Al-Cr database showing a parameter for $PtAl_2$ after further optimisation.

```
PARAMETER G(PTAL2,CR:PT;0)  298.15  -39562.5+62.5*T+0.666*GHSERCR#+
0.334*GHSERPT#;   3000   N REF0 !
```

5. COMPARISON OF EXPERIMENTAL AND CALCULATED RESULTS

The best way to check a "full" database is to recalculate the binary phase diagrams from it, which was successfully accomplished for Pt-Al, Pt-Cr and Al-Cr. The Table 3.13 shows the optimised model parameters, excluding values for parameters that were taken from the COST

[1998Ans] and SGTE [1991Din] databases and Oikawa's Cr-Pt database [2001Oik]). The full database (in TDB-format) can be found in Appendix B. The isothermal sections calculated from this database showed the best fit to the experimental results. They are shown in Figures 4.22 and 4.23.

Table 3.13. The calculated model parameters for Pt-Al-Cr.

Phase	**Constitution**	**Parameter**	**Value** and/or Reference
Liquid	(Al,Cr,Pt)	${}^{0}G_{Al}^{liq}$ - $H_{Al}^{0,fcc-A1}$ (298.15)	**[1991Din]**
		${}^{0}G_{Cr}^{liq}$ - $H_{Cr}^{0,bcc-A2}$ (298.15)	**[1991Din]**
		${}^{0}G_{Pt}^{liq}$ - $H_{Pt}^{0,fcc-A1}$ (298.15)	**[1991Din]**
		${}^{0}L_{Al,Cr}^{liq}$	**[1998Ans]**
		${}^{1}L_{Al,Cr}^{liq}$	**[1998Ans]**
		${}^{0}L_{Al,Pt}^{liq}$	-352536+114.8*T **[2004Pri1, 2004Pri2]**
		${}^{1}L_{Al,Pt}^{liq}$	+68566-53*T **[2004Pri1, 2004Pri2]**
		${}^{0}L_{Cr,Pt}^{liq}$	**[2001Oik]**
fcc-A1	(Al,Cr,Pt)(Va)	${}^{0}G_{Al}^{0,fcc-A1}$ - $H_{Al}^{0,fcc-A1}$ (298.15)	**[1991Din]**
		${}^{0}G_{Pt}^{0,fcc-A1}$ - $H_{Pt}^{0,fcc-A1}$ (298.15)	**[1991Din]**
		${}^{0}G_{Cr}^{0,fcc-A1}$ - $H_{Cr}^{0,fcc-A1}$ (298.15)	**[1998Ans]**
		${}^{0}L_{Al,Cr}^{fcc-A1}$	**[1998Ans]**
		${}^{0}L_{Al,Pt}^{fcc-A1}$	+APL0FCC+ALPTG0+1.5*REC **[2004Pri1, 2004Pri2]**
		${}^{1}L_{Al,Pt}^{fcc-A1}$	+APL1FCC+ALPTG1 **[2004Pri1, 2004Pri2]**
		${}^{2}L_{Al,Pt}^{fcc-A1}$	+APL2FCC+ALPTG2-1.5*REC **[2004Pri1, 2004Pri2]**
		${}^{0}L_{Cr,Pt}^{fcc-A1}$	**[2001Oik]**
		${}^{1}L_{Cr,Pt}^{fcc-A1}$	**[2001Oik]**
bcc-A2	(Al,Cr,Pt)(Va)	${}^{0}G_{Al}^{0,bcc-A2}$ - $H_{Al}^{0,bcc-A2}$ (298.15)	**[1991Din]**
		${}^{0}G_{Cr}^{0,bcc-A2}$ - $H_{Cr}^{0,bcc-A2}$ (298.15)	**[1991Din]**
		${}^{0}G_{Pt}^{0,bcc-A2}$ - $H_{Pt}^{0,bcc-A2}$ (298.15)	**[1991Din]**
		${}^{0}L_{Al,Cr}^{bcc-A2}$	**[1998Ans]**
		${}^{0}L_{Cr,Pt}^{bcc-A2}$	**[2001Oik]**
$Al_{11}Cr_2$	$(Al)_{10}(Al)_1(Cr)_2$	$G_{Al:Al:Cr}^{Al11Cr2}$	**[1998Ans]**
$Al_{13}Cr_2$	$(Al)_{13}(Cr)_2$	$G_{Al:Cr}^{Al13Cr2}$	**[1998Ans]**
Al_4Cr	$(Al)_4(Cr)$	$G_{Al:Cr}^{Al4Cr}$	**[1998Ans]**

Table 3.13. The calculated model parameters for Pt-Al-Cr (contd.)

Al_8Cr_5 (HT)	$(Al)_8(Cr)_5$	$G^{Al8Cr5\_H}_{Al:Cr}$	**[1998Ans]**
Al_8Cr_5 (LT)	$(Al)_8(Cr)_5$	$G^{Al8Cr5\_L}_{Al:Cr}$	**[1998Ans]**
Al_9Cr_4 (HT)	$(Al)_9(Cr)_4$	$G^{Al9Cr4\_H}_{Al:Cr}$	**[1998Ans]**
Al_9Cr_4 (LT)	$(Al)_9(Cr)_4$	$G^{Al9Cr4\_L}_{Al:Cr}$	**[1998Ans]**
$AlCr_2$	$(Al)(Cr)_2$	$G^{AlCr2}_{Al:Cr}$	**[1998Ans]**
Cr_3Pt	$(Cr,Pt)_3(Cr,Pt)$	$G^{Cr3Pt\_A15}_{Cr:Cr}$	**[2001Oik]**
		$G^{Cr3Pt\_A15}_{Pt:Cr}$	**[2001Oik]**
		$G^{Cr3Pt\_A15}_{Cr:Pt}$	**[2001Oik]**
		$G^{Cr3Pt\_A15}_{Pt:Pt}$	**[2001Oik]**
		$L^{Cr3Pt\_A15}_{Cr,Pt:Cr}$	**[2001Oik]**
		$L^{Cr3Pt\_A15}_{Cr:Cr,Pt}$	**[2001Oik]**
		$L^{Cr3Pt\_A15}_{Pt:Cr,Pt}$	**[2001Oik]**
		$L^{Cr3Pt\_A15}_{Cr,Pt:Pt}$	**[2001Oik]**
Pt_5Al_3	$(Pt)_5(Al)_3$	$G^{Pt5Al3}_{Al:Pt}$	-87260+24*T +.375*GHSERAL +.625*GHSERPT **[2004Pri1, 2004Pri2]**
Pt_2Al_3	$(Pt)_2(Al)_3$	$G^{Pt2Al3}_{Al:Pt}$	-89884+21.5*T +.6*GHSERAL+.4*GHSERPT **[2004Pri1, 2004Pri2]**
Pt_5Al_{21}	$(Pt)_5(Al)_{21}$	$G^{Pt5Al21}_{Al:Pt}$	-56873+14.8*T +.8077*GHSERAL +.1923*GHSERPT **[2004Pri1, 2004Pri2]**
Pt_8Al_{21}	$(Pt)_8(Al)_{21}$	$G^{Pt8Al21}_{Al:Pt}$	-82342+23.7*T +0.7242*GHSERAL +.2759*GHSERPT **[2004Pri1, 2004Pri2]**
Beta	$(Pt)_{0.52}(Al)_{0.48}$	$G^{Beta}_{Al:Pt}$	-92723+23.88*T +.48*GHSERAL+.52*GHSERPT **[2004Pri1, 2004Pri2]**
Pt_2Al	$(Pt)_2(Al)$	$G^{Pt2Al}_{Al:Cr}$	10000 +0.334*GHSERAL +0.666*GHSERCR **[This work]**
		$G^{Pt2Al}_{Cr:Pt}$	20000 +0.334*GHSERCR +.666*GHSERPT **[This work]**
		$G^{Pt2Al}_{Cr:Cr}$	150000+GHSERCR **[This work]**
		$G^{Pt2Al}_{Al:Pt}$	-84989+24.9*T +.334*GHSERAL +.666*GHSERPT **[2004Pri1, 2004Pri2]**
		$L^{Pt2Al}_{Al,Cr:Pt}$	-118000+19.9*T **[This work]**

Table 3.13. The calculated model parameters for Pt-Al-Cr (contd.).

		$L^{Pt2Al}_{Al:Pt,Cr}$	-178000+44.7*T **[This work]**
		$L^{Pt2Al}_{Al,Cr:Crt}$	-118000+19.9*T **[This work]**
		$L^{Pt2Al}_{Cr:Pt,Cr}$	-178000+44.7*T **[This work]**
PtAl	(Pt)(Al)	$G^{PtAl}_{Al:Cr}$	20000 +0.5*GHSERAL+0.5*GHSERCR **[This work]**
		$G^{PtAl}_{Cr:Pt}$	35000 +0.5*GHSERCR+0.5*GHSERPT **[This work]**
		$G^{PtAl}_{Cr:Cr}$	200000+GHSERCR **[This work]**
		$G^{PtAl}_{Al:Pt}$	-94071+24.1*T +.5*GHSERAL+.5*GHSERPT **[2004Pri1, 2004Pri2]**
		$L^{PtAl}_{Al,Cr:Pt}$	-187060+65.9*T **[This work]**
		$L^{PtAl}_{Al:Pt,Cr}$	-234908+81.6*T **[This work]**
		$L^{PtAl}_{Al,Cr:Crt}$	-187060+65.9*T **[This work]**
		$L^{PtAl}_{Cr:Pt,Cr}$	-234908+81.6*T **[This work]**
$PtAl_2$	$(Pt)(Al)_2$	$G^{PtAl2}_{Al:Cr}$	+20000 +0.666*GHSERAL +0.334*GHSERCR **[This work]**
		$G^{PtAl2}_{Cr:Pt}$	-39562.5+62.5*T +0.666*GHSERCR +0.334*GHSERPT **[This work]**
		$G^{PtAl2}_{Cr:Cr}$	+170000+GHSERCR **[This work]**
		$G^{PtAl2}_{Al:Pt}$	-87898+23.3*T +.666*GHSERAL +.334*GHSERPT **[2004Pri1, 2004Pri2]**
		$L^{PtAl2}_{Al,Cr:Pt}$	-108000+19.9*T **[This work]**
		$L^{PtAl2}_{Al:Pt,Cr}$	-168000+44.7*T **[This work]**
		$L^{PtAl2}_{Al,Cr:Cr}$	-108000+19.9*T **[This work]**
		$L^{PtAl2}_{Cr:Pt,Cr}$	-168000+44.7*T **[This work]**
T1	$(Pt)_{0.5}(Al)_{0.3}(Cr)_{0.2}$	$G^{TAO\_1}_{Pt:Al:Cr}$	-130000+40.28*T +.5*GHSERPT+ .3*GHSERAL+.2*GHSERCR **[This work]**

Table 3.13. The calculated model parameters for Pt-Al-Cr (contd.).

$L1_2$ (Pt_3Al, Pt_3Cr, PtCr)	$(Al,Cr,Pt)_{0.25}$ $(Al,Cr,Pt)_{0.25}$ $(Al,Cr,Pt)_{0.25}$ $(Al,Cr,Pt)_{0.25}$ (Va)	$G^{L12}_{Pt:Pt:Pt:Al} = G^{L12}_{Pt:Pt:Al:Pt} =$ $G^{L12}_{Pt:Al:Pt:Pt} = G^{L12}_{Al:Pt:Pt:Pt}$	GAL1PT3 **[2004Pri1, 2004Pri2]**
		$G^{L12}_{Al:Al:Al:Pt} = G^{L12}_{Al:Al:Pt:Al} =$ $G^{L12}_{Al:Pt:Al:Al} = G^{L12}_{Pt:Al:Al:Al}$	GAL3PT1 **[2004Pri1, 2004Pri2]**
		$G^{L12}_{Al:Al:Pt:Pt} = G^{L12}_{Pt:Pt:Al:Al} =$ $G^{L12}_{Al:Pt:Pt:Al} = G^{L12}_{Pt:Al:Al:Pt}$	GAL2PT2 **[2004Pri1, 2004Pri2]**
		$G^{L12}_{Pt:Pt:Pt:Cr} = G^{L12}_{Pt:Pt:Cr:Pt} =$ $G^{L12}_{Pt:Cr:Pt:Pt} = G^{L12}_{Cr:Pt:Pt:Pt}$	GCR1PT3 **[This work]**
		$G^{L12}_{Cr:Cr:Cr:Pt} = G^{L12}_{Cr:Cr:Pt:Cr} =$ $G^{L12}_{Cr:Pt:Cr:Cr} = G^{L12}_{Pt:Cr:Cr:Cr}$	GCR3PT1 **[This work]**
		$G^{L12}_{Cr:Cr:Pt:Pt} = G^{L12}_{Pt:Pt:Cr:Cr} =$ $G^{L12}_{Cr:Pt:Pt:Cr} = G^{L12}_{Cr:Al:Al:Cr} =$	GCR2PT2 **[This work]**
		$L^{L12}_{Cr:Cr:Al:Pt} = L^{L12}_{Cr:Cr:Pt:Al} =$ $L^{L12}_{Cr:Pt:Cr:Al} = L^{L12}_{Cr:Al:Cr:Pt} =$ $L^{L12}_{Cr:Al:Pt:Cr} = L^{L12}_{Cr:Pt:Al:Cr} =$ $L^{L12}_{Al:Pt:Cr:Cr} = L^{L12}_{Pt:Al:Cr:Cr} =$ $L^{L12}_{Al:Cr:Cr:Pt} = L^{L12}_{Pt:Cr:Cr:Al} =$ $L^{L12}_{Al:Cr:Pt:Cr} = L^{L12}_{Pt:Cr:Al:Cr}$	ALCR2PT **[This work]**
		$L^{L12}_{Pt:Pt:Al:Cr} = L^{L12}_{Pt:Pt:Cr:Al} =$ $L^{L12}_{Pt:Cr:Pt:Al} = L^{L12}_{Pt:Al:Pt:Cr} =$ $L^{L12}_{Pt:Al:Cr:Ptr} = L^{L12}_{Pt:Cr:Al:Pt} =$ $L^{L12}_{Al:Pt:Pt:Cr} = L^{L12}_{Cr:Al:Pt:Pt} =$ $L^{L12}_{Al:Cr:Cr:Pt} = L^{L12}_{Cr:Pt:Pt:Al} =$ $L^{L12}_{Al:Pt:Cr:Pt} = L^{L12}_{Cr:Pt:Al:Pt}$	ALCRPT2 **[This work]**
		$L^{L12}_{Al:Al:Cr:Pt} = L^{L12}_{Al:Al:Pt:Cr} =$ $L^{L12}_{Al:Pt:Al:Cr} = L^{L12}_{Al:Cr:Al:Pt} =$ $L^{L12}_{Al:Cr:Pt:Al} = L^{L12}_{Al:Pt:Cr:Al} =$ $L^{L12}_{Cr:Pt:Al:Al} = L^{L12}_{Pt:Cr:Al:Al} =$ $L^{L12}_{Cr:Al:Al:Pt} = L^{L12}_{Pt:Al:Al:Cr} =$ $L^{L12}_{Cr:Al:Pt:Al} = L^{L12}_{Pt:Al:Cr:Al}$	AL2CRPT **[This work]**
		$L^{L12}_{Al,Pt:Al,Pt:*:*} = L^{L12}_{Al,Pt:*:Al,Pt:*} =$ $L^{L12}_{Al,Pt:*:*:Al,Pt} = L^{L12}_{*:Al,Pt:Al,Pt:*} =$ $L^{L12}_{*:Al,Pt:*:Al,Pt} = L^{L12}_{*:*:Al,Pt:Al,Pt}$	REC **[2004Pri1, 2004Pri2]**

Table 3.13. The calculated model parameters for Pt-Al-Cr (contd.).

		$L^{L12}_{Cr,Pt:Cr,Pt:*:*} = L^{L12}_{Cr,Pt:*:Cr,Pt:*} = L^{L12}_{Cr,Pt:*:*:Cr,Pt} = L^{L12}_{*:Cr,Pt:Cr,Pt:*} = L^{L12}_{*:Cr,Pt:*:Cr,Pt} = L^{L12}_{*:*:Cr,Pt:Cr,Pt}$	REC2 **[This work]**
		$L^{L12}_{Al,Pt:Al:Cr:Al} = L^{L12}_{Cr:Al,Pt:Al:Al} = L^{L12}_{Pt:Al,Pt:Pt:Cr} = \ldots\ldots$ *See Appendix B for all 79 parameters*	UL0 **[2004Pri1, 2004Pri2]**
		$L^{L12}_{Cr,Pt:Al:Al:Al} = L^{L12}_{Al:Cr,Pt:Al:Al} = L^{L12}_{Pt:Cr,Pt:Al:Al} = \ldots\ldots$ *See Appendix B for all 86 parameters*	UL1 **[This work]**
Functions		GHSERCR	**[1991Din]**
		GHSERAL	**[1991Din]**
		GHSERAL	**[1991Din]**
		APL0FCC	-110531-22.9*T **[2004Pri1, 2004Pri2]**
		APL1FCC	-25094 **[2004Pri1, 2004Pri2]**
		APL2FCC	21475 **[2004Pri1, 2004Pri2]**
		GAL3PT1	+3*UAP **[2004Pri1, 2004Pri2]**
		GAL2PT2	+4*UAP **[2004Pri1, 2004Pri2]**
		GAL1PT3	+3*UAP-3913 **[2004Pri1, 2004Pri2]**
		ALPTG0	+GAL3PT1+1.5*GAL2PT2+GAL1PT3 **[2004Pri1, 2004Pri2]**
		ALPTG1	+2*GAL3PT1-2*GAL1PT3 **[2004Pri1, 2004Pri2]**
		ALPTG2	+GAL3PT1-1.5*GAL2PT2+GAL1PT3 **[2004Pri1, 2004Pri2]**
		GCR3PT1	3120.624 **[This work]**
		GCR2PT2	-8541.7081 **[This work]**
		GCR1PT3	-4610 **[This work]**
		ALCR2PT = ALCRPT2 = AL2CRPT	+83650-55*T **[This work]**
		UL0	+1412.8+5.7*T **[2004Pri1, 2004Pri2]**
		UL1	1500 **[This work]**
		REC	UAP **[2004Pri1, 2004Pri2]**
		REC2	1000 **[This work]**
		UAP	-13595+8.3*T **[2004Pri1, 2004Pri2]**

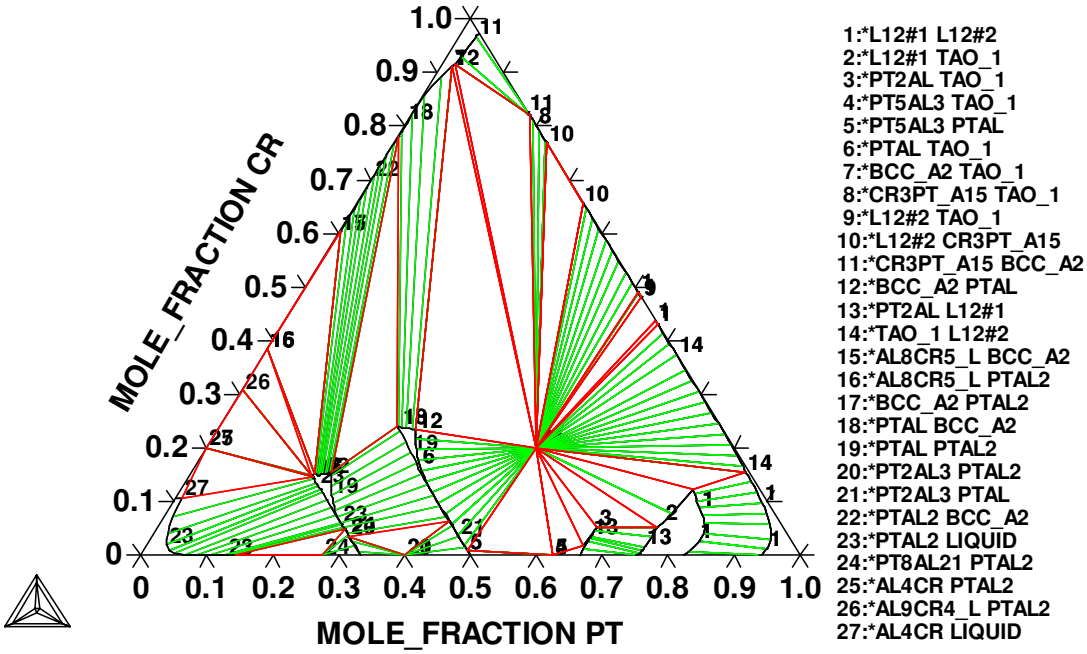

Figure 3.22. Best calculated 1000℃ isothermal section for Pt-Al-Cr.

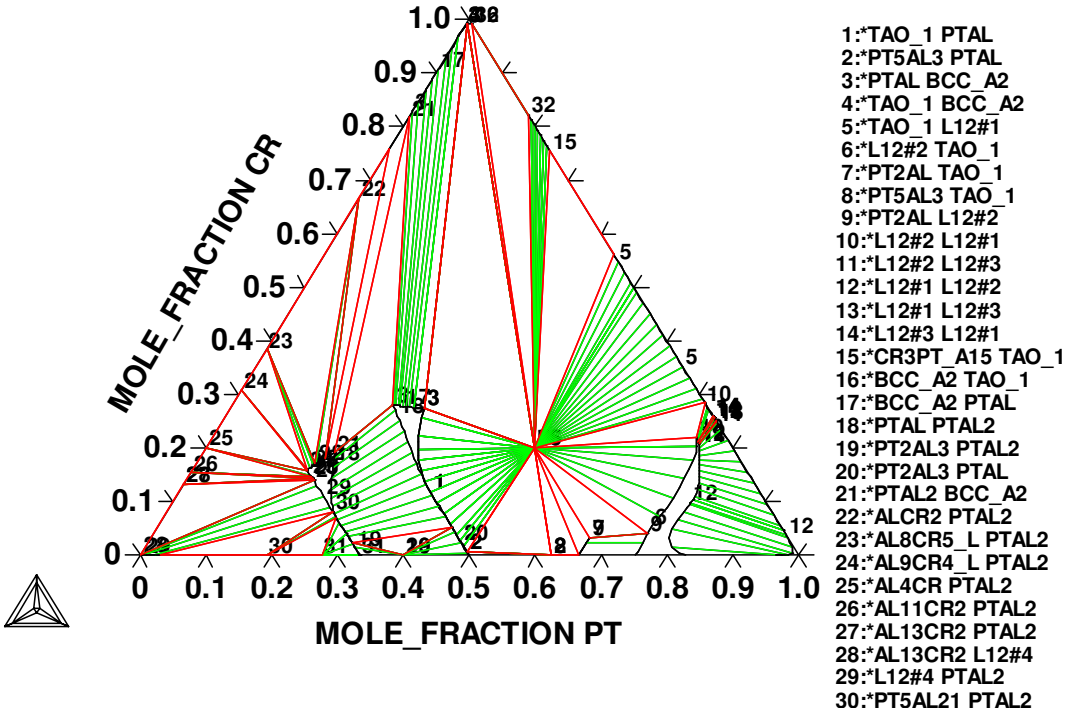

Figure 3.23. Best calculated 600℃ isothermal section for Pt-Al-Cr.

Table 3.14 gives a detailed comparison between the experimental and calculated results.

Table 3.14. Comparison between the experimental and calculated results at 600℃ and 1000℃.

	600°C	**1000°C**
Exact agreement with experimentally determined phase relations	BCC_A2/PTAL2	
	PT2AL3/PTAL	
	PTAL/T1	
	BCC_A2/T1/CR3PT_A15	
	L12(FCC)/L12(Pt_3Al)	
	PT2AL/L12(Pt_3Al)	
	BCC_A2/PTAL	
	AL8CR5/AL9CR4/PTAL2	
	BCC_A2/PTAL2/PTAL	
	PTAL2/PTAL	
	PTAL2/PT2AL3/PTAL	PTAL2/PT2AL3
	TAO_1/PT2AL	TAO_1/PT2AL/L12(Pt3Al)
	CR3PT_A15/T1/CRPT	
	L12(Pt_3Cr)/L12(Pt_3Al)	
	ALCR2/PTAL2	
		LIQUID/PTAL2
Phase relations highly likely to be correct as inferred from experimentally determined equilibria	BCC_A2/PTAL/TAO_1	
	TAO_1/PT5AL3/PT2AL	
	TAO_1/PTAL/PT5AL3	
	AL9CR4/AL4CR/PTAL2	
	AL8CR5/PTAL2	AL8CR5/AL9CR4/PTAL2
		BCC_A2/AL9CR4/PTAL2
		BCC_A2/ CR3PT_A15
	CR3PT_A15/TAO_1	CR3PT_A15/TAO_1/L12(CrPt)
	L12(CrPt)/TAO_1	L12(CrPt)/TAO_1/L12(Pt_3Cr)
		TAO_1/L12(Pt_3Al)
		TAO_1/PT2AL
	AL4CR/ AL11CR2(Al_5Cr)/PTAL2	AL4CR/LIQUID
		AL4CR/LIQUID/PTAL2
	PT8AL21/PTAL2	
	PTAL2/PT5AL21/ PT8AL21	
	PTAL2/L12(Al)/PT5AL21	
	PTAL2/L12(Al)	
	AL13CR2/L12(Al)/PTAL2	
	AL11CR2(Al_5Cr)/ AL13CR2/PTAL2	
	ALCR2/AL8CR5/PTAL2	
Bad agreement with experimentally determined phase relations		PTAL2/PTAL
		PTAL2/PT2AL3/PTAL
		BCC_A2/ PTAL2/PTAL
		L12(Pt_3Cr)/TAO_1
	TAO_1/L12(Pt_3Al)	L12(Pt_3Cr/(Pt))/TAO_1/L12(Pt_3Al)
Other comments	Direction of extension incorrect for PTAL2, PTAL and PT2AL	
	The stability range of the ordered and disordered fcc regions ((Pt), Pt_3Cr, CrPt) too narrow	
	Extension of PT2AL too little	
		Extension of PTAL too much
	Extension of L12 (Pt_3Al) too much	Extension of L12 (Pt_3Al) much too little
	The stability range of BCC_A2 too narrow	

When comparing the experimental and calculated results, it is clear that the adavantages outweigh the disadvantages where the calculation is concerned. Many equilibria are in exact agreement with what was observed experimentally. Many equilibria, especially three-phase relations that were not directly observed experimentally, seemed highly plausible when taking the related two-phase equilibria into account that had been observed experimentally. In fact, the calculated isothermal sections were a great help in completing the diagrams in those areas where experimental samples had not been examined. A specific example of this is the establishment of the Al-rich corner of the 600°C isothermal section. Because alloys with more than ~75 at.% Al were brittle in the as-cast condition and shattered during the process of breaking them out of the mount, none of the alloys were annealed at 600°C, and the as-cast results were shown in the experimentally determined section, with not much information. On the other hand, the calculated 600°C section gave a much clearer picture. This was of great importance in obtaining a much better understanding of the Pt-Al-Cr system, without having to prepare more samples to do time-consuming phase characterisation. This is very illustrative of the practical importance of the CALPHAD technique of predictive calculation.

There were some problems as well. These were mainly related to the extent and the direction that the Pt-Al compounds extended into the ternary. From the description in the previous section it was obvious that

- the specific model that was used did not allow the direction to be changed, only the extent, but that
- the amount of extension of these compounds could not be manipulated independently.

At this stage this cannot be improved upon with regard to the experimental data without adversely affecting other phase relations.

Since $PtAl_2$ and PtAl were forced to be thermodynamically stable, the relative stability of Pt_2Al_3 was affected, and that is the reason why the equilibria in that region were inconsistent with the experimental results at 1000°C. In similar fashion, the forced stability of T1 affected that of Pt_2Al, and the latter cannot be made more stable without resulting in a drastic divergence from the experimental diagrams. The current results are therefore the most satisfactory. Considering that the database was optimised manually, would raise the question whether it could be improved by using Thermo-Calc optimisation module, PARROT. Sadly, the answer is no. Several POP-files were created: a master one, including most of the

experimentally-observed equilibria; one for only Pt-Al compounds; and one for equilibria involving L12 only. None of these converged towards a satisfactory optimisation, and the results were always worse that those seen in Figures 4.22 and 4.23. This was definitely an indication that the database had some problems.

The fact that the stability range of Pt_3Al, (Pt), Pt_3Cr and CrPt were inconsistent with regard to the experimental results clearly showed that the model description for L12 was problematic. It is, unfortunately, a very complex description, and to date many parameter values were still taken as identical or zero for reasons of simplification, and therefore not necessarily correct. The problems with the L12 description were underlined when an attempt was made to calculate a liquidus surface projection for the system with the latest database.

Making use of the TERN module of TCC-R for automatic calculation of the liquidus surface projection, was an utter failure. Using manual commands in the POLY module and using many different starting points, a partial surface was calculated (Figure 3.24(a)). An attempt was also made to calculate the liquidus surface using Pandat. This was more successful, especially for > 50 at.% Al. However, it was very obvious that the software could not cope with the description for L12, because the >40 at.% Pt region was totally incoherent (Figure 3.24 (b)).

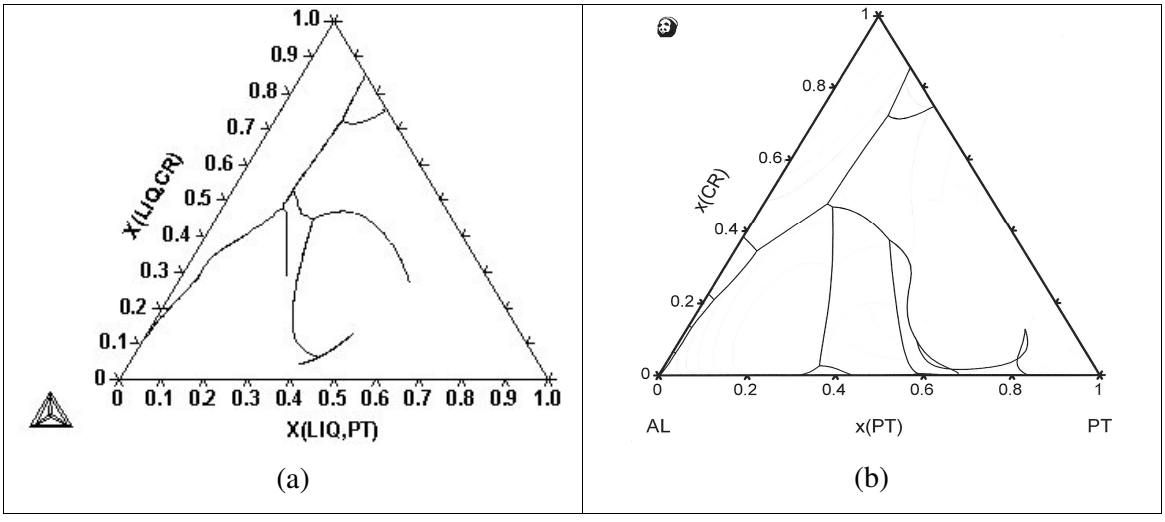

Figure 3.24. Partial liquidus surfaces for Pt-Al-Cr calculated using (a) TCC-R, and (b) Pandat.

A composite liquidus surface projection was created from the most likely lines of Figure 3.24 (a) and (b), and the result (Figure 3.25 (a)) was compared to the experimentally determined liquidus surface (Figure 2.140, shown again in Figure 3.25 (b) for easy reference).

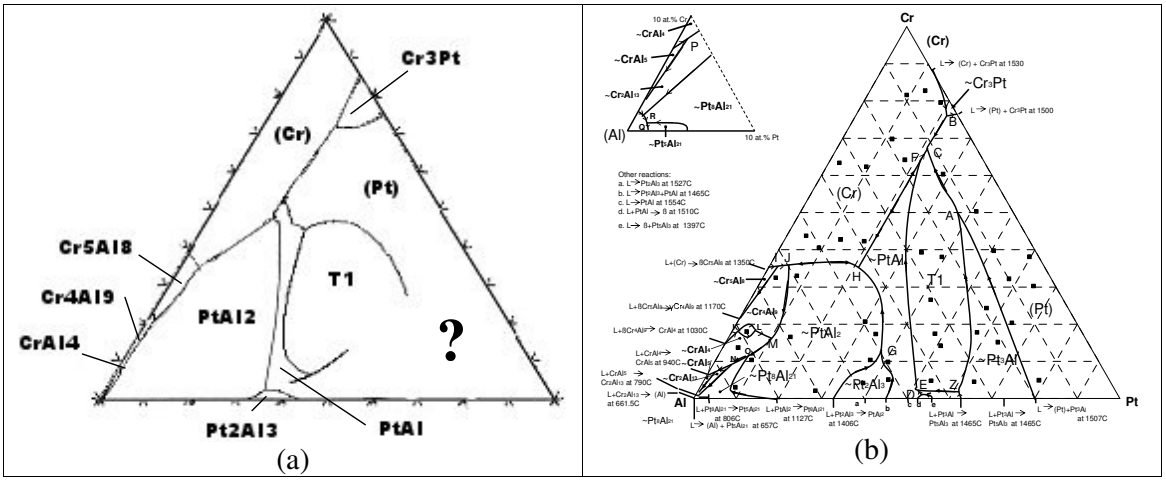

Figure 3.25. (a) Composite liquidus surface projection created from calculations by TCC-R and Pandat, compared to (b) the experimentally determined liquidus surface projection (this work).

Except for the Pt-rich corner, the agreement between the experimentally derived and calculated liquidus surface projection was good. These calculated results were in fact a vast improvement on the calculation done earlier using extrapolation only (Figure 3.12 (a)). The Cr_3Pt, (Cr), $PtAl_2$, Pt_2Al_3 and PtAl surfaces were particularly well calculated. The position of the T1 surface was much better than before. The reason why the Al-rich corner was different from the experimentally derived one was primarily the result of alloy Pt_3:Al_{79}:Cr_{18}, which showed the primary solidification of ternary T3≈$CrAl_3$ which was not modelled *per se* (but is mathematically and rightfully part of the L12 description), and alloy Pt_3:Al_{65}:Cr_{32}, which showed that the liquidus surface for ~Cr_4Al_9 extended to higher Cr-levels than one would have expected, resulting in a much smaller liquidus surface for ~Cr_5Al_8.The failure in the Pt-rich corner is likely to be due to the model used, and the insufficient data available to optimise it.

6. CONCLUSIONS AND RECOMMENDATIONS

Overall, the results of the modelling of the Pt-Al-Cr system using Thermo-Calc were good. The database could definitely be used to get a very good prediction of phase relations between 600°C and 1000°C, and even up to temperatures close to the melting point, reasonable results would be obtained. The results complimented the experimental work significantly and the value of the CALPHAD method as a tool in alloy design has been clearly demonstrated. However, the match between the calculated and experimental diagrams could be improved and more work is definitely necessary, but it falls outside the scope of this thesis.

Most of the problems pertain to the Al-Pt compounds and the ordered and disordered (L12) fcc phases, which involves both the Al-Pt and Pt-Cr binary systems. Problems with these binary diagrams have been mentioned before. There is still uncertainty about the exact nature of the ordering reactions in Pt_3Al as well as its stability range. The stability range of Pt_2Al is also questionable. Work is undergoing to answer some of these questions [2006Tsh]. Anomalies in the Cr-Pt system have already been recognised by Süss et al. [2006Süs1] and Nzula et al. [2005Nzu] and also in this work with regard to the eutectic temperatures, but the biggest problem remains the compositions and temperatures of the order-disorder reactions in the system. The new work by Zhao et al. [2005Zha] showing a much more sensible diagram (Figure 1.2) underlines the fact that the system needs more attention. It is therefore recommended to:

- Undertake slow scanning rate DTA for samples in the Cr-Pt and Cr-Ru systems to obtain reaction temperatures.
- Undertake phase diagram studies in the Cr-Pt and Cr-Ru systems to obtain better phase equilibria data.
- Consider the use of differential scanning calorimetry (DSC) to obtain thermodynamic values (enthalphy of formation) for phases in the Pt-Al-Cr and Pt-Cr-Ru systems.
- Consider reassessing the Cr-Pt model with regard to Zhao's results and evaluating the effect on the overall system.

As with the Cr-Pt-Ru system, problems with the constituting binary systems seem to be the major cause for problems encountered in the modelling. Currently, it would be a waste of

time to optimise the databases (both Pt-Al-Cr and Cr-Pt-Ru) for the intermetallic phases any further because there are too many unknowns. Only once the Al-Pt and especially the Cr-Pt and Cr-Ru binary phase diagrams are confirmed more rigorously, the ternary calculated phase diagrams could be worked on with more confidence, which should make extrapolation into the quaternary not only easier, but also more valid.